IEEE Access
Multidisciplinary | Rapid Review | Open Access Journal

Received 14 June 2023, accepted 7 July 2023, date of publication 14 July 2023, date of current version 3 August 2023.

Digital Object Identifier 10.1109/ACCESS.2023.3295329

RESEARCH ARTICLE

A Perfect Challenge to Select the Ideal Virus Vaccine Using a New Potent Hierarchical Algorithm in a Smart Laboratory

EL MILOUD AR-REYOUCHI[1], (Senior Member, IEEE), GUNJAN VARSHNEY[2], (Senior Member, IEEE), KAMAL GHOUMID[3], (Member, IEEE), FABIEN PICAUD[4], GUILLAUME HERLEM[4], AHMED MOSTEFAOUI[5], AND RÉDA YAHIAOUI[4]

[1]Department of Telecommunication and Computer Science, ETS, 28012 Madrid, Spain
[2]Department of Electrical Engineering, JSS Academy of Technical Education Noida, Noida, Uttar Pradesh 201301, India
[3]Department of Electronics, Informatics and Telecommunications, ENSAO, Mohammed First University, Oujda 60050, Morocco
[4]NanoMedicine Laboratory, Therapeutic, Imagery, Franche-Comte University, 25030 Besançon, France
[5]Disc Department, FEMTO-ST Institute, University of Franche Comte, 90000 Belfort, France

Corresponding author: Kamal Ghoumid (k.ghoumid@ump.ac.ma)

This work was supported in part by the FEDER "European Regional Development Fund" Project "Reper@ge" (The Reper@ge Project is developed with the Nanomedicine, Imaging and Therapeutics Laboratory, Franche-Comté University); and in part by the Engineering Sciences Laboratory (LSI), ENSAO, Mohamed Premier University, Oudja, Morocco.

ABSTRACT Improving the bit error rate (BER) in dense wireless medical sensor networks (WMSNs) using small areas is challenging. Ensuring the relay of big data in healthcare, such as human virus vaccine signs, is always a huge challenge. This paper proposes a new potent hierarchical algorithm (PHA) for controlling several vaccine types in real-time using a uniquely challenging laboratory before being recommended and authorized. This healthcare research paper offers a new medical application in the virus testing communication of several separate and independent patient groups (subnets), exploiting a smart laboratory. The health data aggregator (HDA) nodes of the patients are wirelessly connected to a relay network (RN) via the central node (CN). We develop an efficient communication scheme, improving BER values versus signal-to-noise ratio (SNR), proposing a PHA that requires three main creation stages. The first stage is responsible for collecting big medical data. In the second and third stages, we use coding approaches based on network coding (NC) and low-density parity-check code (LDPC). The proposed PHA reduces BER in deep fading environment receivers for different creating parameters. This paper introduces an innovative approach to tracking the evolution of virus vaccines by integrating IoMT, Big Data, and Artificial Intelligence (AI). This integration enables identifying and selecting the optimal and most effective vaccine.

INDEX TERMS Big data, medical wireless network communications, network coding, BER, LDPC, Internet of Medical Things, artificial intelligence.

I. INTRODUCTION

Rapidly evolving viruses present new possibilities for transforming healthcare by developing advanced medical devices, protocols, and algorithms. Ensuring fair access to safe and effective vaccines is crucial for ending the COVID-19 pandemic. Therefore, concurrently testing and developing numerous vaccines in a single, smart laboratory is highly promising and encouraging. In this context, "smart laboratory" typically refers to a physical laboratory equipped with advanced technologies such as IoMT devices, sensors, automation systems, AI, and data analytics tools. The focus is on leveraging these smart technologies to optimize the vaccine selection process, improve experimental procedures, and enhance vaccine development's overall efficiency and accuracy.

The associate editor coordinating the review of this manuscript and approving it for publication was Sathish Kumar.

The full packet reception in IoMT applications for mission-critical wireless communication is a big challenge. The problem is further complicated for small surfaces containing large quantities of patients. The ultimate goal of designing a wireless network communication system is to communicate instantaneously and efficiently [1] with users between several dense and separate subnets over a wireless bridge. Establishing communication between several or two networks via a single RN [2] requires high-level skills at their connection point. This setup is widely utilized in wireless cellular networks where the two cells cannot communicate directly without an intermediate or a relay node [3].

The multiple source patient nodes and multiple destinations patient nodes cannot communicate, with each other, directly in such a network. This lack of reception can be due to the obstacles separating the HDA patient group's areas by the large or short distance between the multiple source nodes and the multiple destination nodes exceeding the transmission range. The proposed algorithm allows IoMT devices to provide a reliable service for mission-critical applications, especially to test the performance of the different types of virus vaccine, namely coronavirus 2019 (COVID-19). NC can enhance throughput in various scenarios, including unicast, multicast, and broadcast transmissions. Furthermore, in multi-rate situations [4], NC continues to exhibit impressive performance gains when applied twice. NC can also be seamlessly integrated into wireless communication protocols, algorithms, and strategies to improve the BER effectively [5], [6]. The role of BER is pivotal in optimizing the performance of IoMT networks operating in densely populated and spatially constrained environments. Additionally, NC proves beneficial in enhancing the reliability and speed of data gathering in smart grids [7] and WMSNs [8]. To achieve efficient real-time communication, it is crucial to implement an effective combining scheme [9] at the RN. NC has traditionally been utilized in multicast transmissions to increase network capacity [10], [11] and improve RTT (Round Trip Time) [12]. However, we employ NC to minimize the BER in our analysis, using the diversity that can induce nodes in a dense network to listen to their neighbors' messages used in [13]. We utilize an ANCC (Adaptive Network Coded Cooperation) coding scheme using the LDPC codes [14], [15]. Gallager [16] proposed LDPC as a fundamentally new technique for error correction in cable, wireless, and optical communications. The LDPC message-passing method is defined by the large, dense parity-check matrix required for its implementation. LDPC coding offers several advantages compared to other techniques like Viterbi and Turbo codes. It provides high coding gains and lower computational complexity, making it an attractive choice for improving the BER in communication systems. LDPC coding outperforms schemes like Reed-Solomon codes when achieving a lower BER. The BER serves as a metric for evaluating the quality and reliability of a communication system. It quantifies the number of erroneous bits transmitted or received relative to the total number of transmitted bits. A lower BER indicates higher accuracy and reliability in data transmission. LDPC codes allow errors to be corrected, and the network becomes responsible for encoding the transmitted data. This helps lower the BER, thereby enhancing the reliability of the communication system. Research studies, as referenced by [17] and [18], support the effectiveness of LDPC codes in reducing the BER and improving overall system performance. Furthermore, because the BER falls as the number of hops required to reach the destination increases, we suggest a system that reduces the number of hops to two, resulting in a tree stages hierarchy.

We plan at BER versus SNR curves, on the one hand between aggregators nodes and CNs, and on the other hand between CNs and the relay network node, which is the last responsible for collecting and processing big data. The NC is interested in the latest and most high-performance techniques to recover lost packets [19], improve BER, and minimize communication delays for wireless IoT networks.

In the proposal, we can use NC to share data by reducing retransmissions when several patient groups' networks connect through the RNs. During transmission, packet loss occurs in a wireless communication system, possibly due to channel noise or when packets arrive at the destination after a long delay.

The successful execution of a multi-dose vaccine program relies on robust coordination among voluntary patients in a laboratory and efficient interactive communication from providers. This guarantees that patients receive and complete their immunizations. Various vaccines are being administered, including AstraZeneca, Pfizer, Sinopharm, Moderna, Johnson, and others.

WSNs are constructed from enormous, low-power sensor nodes that can perceive, analyze, and transfer big data. These sensor nodes monitor the phenomenon at various locations, collaborate, and relay the collected data to the base station (BS). . It involves communication between central nodes and the big data-processing relay node. Communication is split into three stages: the first stage collects medical information from the patients of each group. The second stage sends big medical data from the grouping nodes to their central node, and the third stage sends big medical data from the central nodes to the relay node.

The hierarchical algorithm PHA is generally based on network coding with LDPC; it works through HDAs (IoT devices) with built-in sensors that connect to the Internet via the central nodes, and RN then shares data to a platform that applies analytics and shares the information with the testing applications designed to address medical-specific needs. The PHA guarantees a QoS level for finding and returning lost information packets at the vaccine testing lab level. The proposal PAH, designed for healthcare applications such as WMSNs and virus vaccine testing, can

also be applied to address practical problems like traffic congestion. Its primary objective is to improve BER in dense wireless networks and ensure reliable communication efficiency for large medical data, whether in fixed or mobile scenarios. The algorithm effectively reduces BER, particularly in receivers experiencing deep fading environments.

This research paper proposes a real-time PHA to control multiple virus vaccine types in a smart laboratory. The algorithm aims to improve the BER in dense wireless medical sensor networks and ensure reliable data relays in healthcare. The PHA consists of three stages: collecting medical data, using NC and LDPC for coding, and reducing BER in receivers in fading environments. The algorithm utilizes the IoMT to track vaccine evolution and select the best one. The study emphasizes the importance of effective communication schemes, network coding, and LDPC coding in improving BER and reducing delays in wireless IoT networks. The results show promising performance gains and coding advantages compared to non-coding scenarios. It recommends using groups or subnets with many nodes for better system performance. This research contributes to healthcare communication systems and vaccine testing in smart laboratories. This research aims to advance medical wireless networks, specifically WMSNs, by improving the BER in densely populated IoT environments while selecting the optimal vaccine without side effects. The proposed hierarchical algorithm with LDPC and NC in relay networks enhances data transmission.

The rest of the document is structured as follows: Section II overviews related work and discusses research contributions, objectives, and challenges. Section III presents the general model and an overview of the suggested model, providing the basis for the detailed description of the proposed algorithm. Section IV provides a general description of the implementation of the first stage. Section V describes the second stage of the proposed hierarchical algorithm. The suggested hierarchical algorithm's third stage is described in Section VI. The results are provided in section VII. Finally, conclusions are given in Section VIII. Fig. 1 depicts a diagrammatic view of the contents of this paper on healthcare.

II. RELATED WORKS, RESEARCH CONTRIBUTION, OBJECTIVES, AND CHALLENGES

This section reviews related works to identify gaps, highlight improvements, and establish a research foundation. Next, we outline our study's specific research contribution, emphasizing its unique perspective, methodology, or innovation in addressing the identified gaps. We define research objectives to ensure a purposeful and coherent study, providing clear directions and milestones. Acknowledging the inherent challenges, we proactively address potential hurdles, enhancing rigor and reliability for meaningful outcomes. Finally, we provide a comprehensive summary of abbreviations and symbol notation.

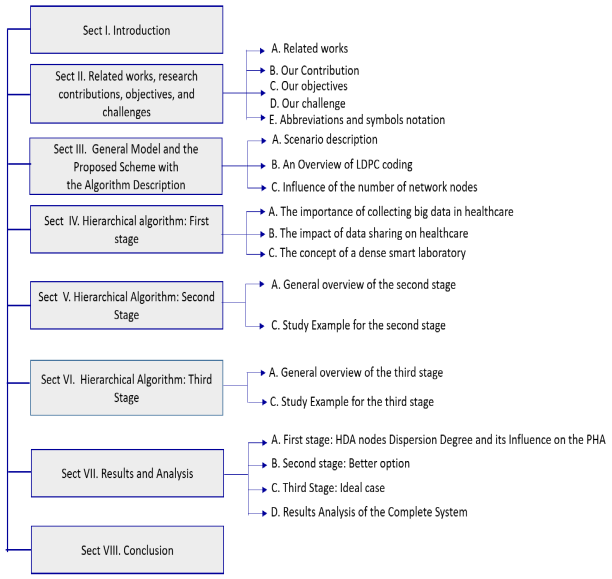

FIGURE 1. The structure of the proposed healthcare.

A. RELATED WORKS

In dense wireless networks and small areas, ensuring the reliable transmission of large medical data is paramount. In this context, Forward Error Correction (FEC), Automatic Repeat Request (ARQ), and Hybrid ARQ (HARQ) techniques play a vital role. These techniques effectively mitigate errors, improve the bit error rate (BER), and ensure the accurate and timely delivery of medical data, thereby enhancing the overall effectiveness of communication systems. Various packet processing methods are available to address the issue of lost or dropped packets during their initial transmission in wireless networks. These methods provide suitable suggestions for recovering lost or dropped packets. In [20] and [21], the authors evaluate the transport protocols' packet-level, FEC, ARQ, and HARQ performance. They focus on data transmission reliability, considering a limited number of authorized retransmissions. But do not examine and determine their performance. Nevertheless, FEC is not the only way for the error control scheme, but it is often combined with another system, like ARQ [22]. Two relevant classes of FEC codes are convolutional codes and block codes. Some work has especially shown that NC can allow guaranteeing the packet's transmission service quality (QoS) [23], [24]. This guarantee is obtained thanks to the simultaneous processing of multiple packets in a coding node allows for improving several parameters in the queues compared to classic routing. In wireless communication networks, extensive scientific research has shown that network coding in two-way relay systems [25] can significantly improve the communication capabilities of wireless links. The research publications [26], [27], [28] provide useful NC with multi-hop traffic flows. A simple combination technique by NC [29] can provide many potential gains to the IoT network. NC improves network delay metrics [30], increases throughput, minimizes forwarding delay, and gives

many benefits to the network, as shown in [30]; also, it can provide an efficient transmission paradigm in network scenarios [31]. This technique originates and sends linear combinations of some original packets in a given generation. Binary addition is carried out over a Galois field (GF); therefore, a linear combination of several packets has the identical size as a single packet. When propagation conditions begin to degrade, many retransmissions are necessitated to successfully transmit the big data, resulting in a significant increase in latency and reduced throughput. To reduce the error and loss effects seen in wireless Internet applications, the authors of [32] provide a novel method that combines word interleaving, FEC, and ARQ. Nevertheless, in [33], the authors provide an overview of the IoMT, emphasizing other protocols and application issues. Shannon [34] developed the information theory to quantify the information loss in transmitting a message. Generally, the random linear network coding (RLNC) system requires that packets be assembled into numerous successive batches with the same fixed size, called generations. The concept of generation was introduced and presented in [35]. The size of the generation and its generation considerably affect the performance of NC [36]. Generations help use the NC at the intermediate station and minimize the complexity of the decoding process. The computation over a decoding matrix with a fixed size is quite simple [34]. Native data is only decoded after all packets are reached correctly, causing an extended forwarding and decoding delay beyond the required time. Moreover, coded packets in a generation must be decoded successfully before packets in a newer generation can be transmitted [37]. The retransmission of the discarded generation (caused by many factors, e.g., original short packets) rears an additional decoding delay.

The main limitation that generations introduce is the high decoding delay. We can also mention the potential information loss due to the whole generation discard, especially with fixed redundancy control (i.e., redundant traffic is adjusted into the network at pre-set time intervals) [6], [35], [38]. The decoding of the generation that comes right after the decoded generation at the destination has to wait for sufficient packets to perform the decoding process, leading to a high decoding delay. Because there are short packets to perform the decoding, generation 2 is discarded. Many propositions [39], [40] introduce a minimum redundancy level to ensure that the generation discard does not happen. However, this may introduce over-redundancy applications. Packet retransmission procedure with the cooperation of network coding for a one-to-many node using a single-hop is a still new field of investigation, first suggested by D. Nguyen et al. [41]. It was further elaborated in [42] by D. Nguyen et al. The authors show bandwidth success achieved in [43]. Using simulation work, they use NC for packet retransmission over classical ARQ protocol. In [22], the authors focus on efficient methods for improving the reliability of packet retransmission in real operational wireless communications. Their analysis concentrates on ACK (Acknowledge) and FEC for efficient transmission performance of different message sizes without introducing network coding by comparing various packet-research algorithms for packet retransmissions. By contrasting several packet coding techniques for packet retransmissions, the authors in [44] carry on the work that had previously started in [41]. While in [45], the authors present analytical research in improving performance, reliability, and Enhancing Sensing in a loss and noisy environment of network coding compared with ARQ and FEC in a loss packet network. The proposed Network Coded Piggy Back (NCPB) takes up NC [46]. It is based on many-to-many reliable network models and developed to suit the real-time constraints of game network applications. The authors in [47] developed an efficient retransmission scheme using XOR-based network coding for wireless broadcast/multicast applications. However, it uses an inefficient and costly reception report scheme and does not consider the effect of heterogeneous and time-varying wireless conditions and fairness. In [19], the authors propose a new NC model with two new mechanisms to recover lost packets that minimize the number of transmissions required to recover from packet loss. Comparing our results with the algorithm [45], the most closely related work is preferable. The proposed mainly concentrates on introducing an efficient NC-founded retransmission algorithm for a many-to-one two-hop network.

B. OUR CONTRIBUTION

This research paper presents a groundbreaking scientific contribution to medical wireless networks, specifically focusing on WMSNs [48], [49]. Employing a hierarchical algorithm enhances the BER in densely populated IoT device environments, aiming to identify the optimal vaccine without any negative side effects. This innovative research enables us to assess and carefully select the most suitable vaccine from a set of options within a single laboratory and represents a pioneering milestone in this unique approach. The unique aspect of this paper lies in the application of NC in relay networks within the medical domain. Previous works, such as [44] and [50], have not proposed an NC-based retransmission scheme that incorporates rapid strategies and considerations of packet latency. This research presents a departure from the traditional coding rules [51], [52], indicating that precise adherence to those rules is no longer necessary. This relaxed coding practice opens possibilities for modifying and developing alternative network coding techniques. By implementing a robust algorithm based on NC, the research significantly improves relaying assured packets in our specific context. It revolutionizes how relay networks operate within the medical field and offers promising advancements in medical wireless networks. In brief, the scientific contribution of this research lies in introducing a hierarchical algorithm that enhances BER in small, dense IoT device environments, specifically in medical wireless networks. It pioneers NC in relay networks within the

medical domain, resulting in remarkable gains and promising opportunities for further development.

C. OUR OBJECTIVES

This paper proposes a scheme to choose the most appropriate and effective vaccination without side effects from a group of vaccines. This selection is among a group of vaccines to select the best. For this, an algorithm based on three stages of hierarchy is proposed, dividing the nodes into groups (subnets) encompassing a fixed number of nodes so that the nodes can establish neighborhoods and directly link with the central node. In this way, communication is based on three stages:

- The first stage corresponds to collecting medical information.
- The second stage corresponds to sending data from the aggregator's nodes to the central node.
- The third stage corresponds to communication between the central nodes and the relay network in charge of data processing.

It seeks to be able to design a WMSN based on the proposed algorithm, obtaining for it the appropriate patient number of groups and the appropriate value of the parameters involved in the system. Coding techniques based on NC and LDPC codes will reduce the BER within each stage. A series of scenarios will be simulated to compare several cases and obtain the parameters for which our algorithm offers the best results. This analysis will be carried out by comparing different curves that present the BER against different values of SNR for each scenario.

D. OUR CHALLENGES

There are safe and efficient vaccinations that provide excellent protection against severe diseases. Our challenge is to select an appropriate vaccine by creating a new reliable communication, flexible networking, and unified platform with large interference in a small area with several patients. Another challenge is to create a perfect medical transmission and reception network without errors in a dense laboratory with several patients in a small area. The proposed algorithm is a kind of decision-making mind based on artificial intelligence to make a parallel difference in the quality of the chosen vaccine. We can then receive decisive comparison results of life or more to save the world population from deadly diseases. This paper proposes an NC-based scheme for an IoT scenario where one RN exchanges medical big data with multiple network monitor nodes over a wireless channel. The problem is the loss of packets transmitted from the central node to manage, control, and monitor patients on a network. We propose an NC with LDPC for retrieving and recovering lost packets and improving BER. The proposed algorithm works for lost retransmission detection and correction.

E. ABBREVIATIONS AND SYMBOLS NOTATION

To ensure consistency, eliminate ambiguity, and maintain a professional tone, it is essential to provide a comprehensive summary of abbreviations and symbol notation in this paper. The summary is presented as follows.

BER	Bit error rate.
WMSN	Wireless medical sensor network.
PHA	Potent hierarchical algorithm.
HDA	Health data aggregator.
RN	Relay network.
CN	Central node.
SNR	Signal-to-noise ratio.
NC	Network coding.
LDPC	Low-density parity-check code.
LDGM	Low-Density Generator Matrix.
IoMT	Internet of Medical Things.
ANCCT	Adaptive Network Coded cooperation.
FEC	Forward Error Correction.
ARQ	Automatic Repeat Request.
HARQ	Hybrid Automatic Repeat Request.
TDMA	Time Division Multiple Access.
WBAN	Wireless body area network.
MATLAB	Matrix LABoratory.
DD	Degree of dispersion.
N	Total number of nodes in a subnet.
N_i	Total number of nodes in subnet i.
P	Parity matrix.
P^T	Transposed matrices of P.
G	Generating matrix.
H	Parity check matrix.
H^T	Transposed matrices of H.
I_N	Identity matrix.
p	Packet.
m	Number of subnets.
n	Number of HDA nodes.
h	Number of hops to reach the destination.
c	Coded word.
s	Syndrome vector.
k	Number of ones in each row.
e	Combined received packet number.
μ	Information vector.
α	Number of bursts per node of each subnet.
β	Number of packets per burst.
T_c	Channel coherence time.
T_s	Taken Time to transmit one packet.
T_β	Bust duration.

III. GENERAL MODEL AND THE PROPOSED SCHEME WITH THE ALGORITHM DESCRIPTION

This section provides an in-depth analysis and comprehensive description of the proposed problem-solving algorithm, outlining each step clearly and systematically.

A. SCENARIO DESCRIPTION

We consider a vaccine testing laboratory, including several subnets. Each subnet comprises volunteer groups vaccinated against viral illnesses for the first time, including COVID-19.

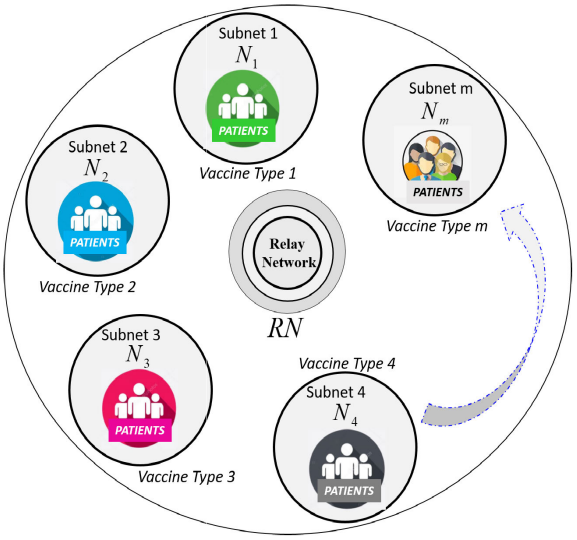

FIGURE 2. Vaccine types: Overview of a vaccine testing laboratory including several subnets. Each subnet owns a type of viral vaccine with its voluntary patients.

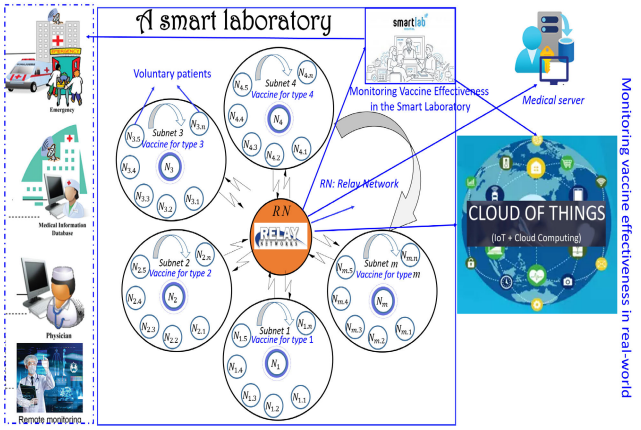

FIGURE 3. The smart laboratory contains *m* groups that communicate among themselves via a relay. Each group comprises *n* advanced HDA nodes that harvest the symptoms that represent the patient's complaints and communicate with one another via a CN.

The communication system is established between several subnets via the RN, as illustrated in Fig.2.

Fig.2 provides a simplified overview of a specific application domain for the proposed algorithm. It compares a set of currently used and other vaccines within the same test laboratory. Our objective is to track the condition of each vaccinated patient, ensuring participant safety by utilizing medical big data and evaluating associated risks. We employ a robust hierarchical algorithm that partitions patients into subnets labeled $1, 2, 3, \ldots, m$. This approach enables us to assess the effectiveness of each vaccine, allowing the laboratory to identify the most suitable vaccine for the population by evaluating various vaccinia viruses. Additionally, we consider the communication system between the RN and the subnets $1, 2, 3, \ldots, m$. Fig. 3 provides a detailed overview model of a critical application domain of the proposed algorithm.

The proposed scenario creates communication between subnets $1, 2, 3, \ldots, m$ IoT nodes and RN; these nodes cooperate to guarantee the transmission of any node to its destination. For most virus vaccine types, the main purpose of the suggested application in this paper is to obtain verifiable information about virus vaccine seekers, such as their efficiency. We need concrete steps using a WMSN-type network structure with three stages to achieve this goal. To further enhance the quality of the information obtained in the second and third stages, a distributed channel coding approach that combines NC and LDPC will be implemented.

The three main stages are involved in creating the proposed *PHA*. A new index for computing a patient's node importance is presented in the proposed algorithm. A heuristic approach is the best approach to finding optimal answers to this problem in medium and large dimensions. The first step is to gather all of the healthcare data. The second step is to set up central nodes. The third step is to relay the information. The results of this approach confirmed that the proposed methodology is applicable.

One of the main problems with wireless communications is that the air is a channel that makes transmissions quite difficult, notably increasing the number of errors compared to wired networks. Broadcasting big medical data over a wireless network is often accomplished via antennas in RN. Most antennas are very small pieces of hardware that are built into IoT medical devices. Our scenario necessitates two transfers to reach the RN. The connection between HDA and CN requires one hop. Also, the wireless connection between CN and RN needs one more hop. In a multi-hop scenario, the BER is calculated as the sum of the probabilities that any of the hops will have errors, even if the data was received correctly in the previous hops:

$$BER_{tot} = \sum_{i=1}^{h} BER_i(\prod_{n+1}^{h}(1 - 2BER_j) \tag{1}$$

where BER_{tot} represents the BER, BER(i) represents the BER that occurs in hop number i, and h represents the total number of hops required to reach the destination. If equation (1) is worked out for a situation with two hops, we find that:

$$BER_{tot} = BER_1 + BER_2 - 2BER_1.BER_2 \tag{2}$$

where BER_1 and BER_2 are the second and third-stage error probabilities, respectively.

In a shared medium, it is very important to develop a method that guarantees that all the nodes that share that medium can transmit. In addition, interference between the different nodes must be reduced as much as possible. In our case, our scenario comprises many nodes that want to transmit information to a common destination. To simplify the work of the nodes, the access mode to the medium to be used will be TDMA access (Time Division Multiple Access or Multiple Access by Division in Time). When using

TDMA, each node is assigned a specific space or time slot to send its data, while the rest remain silent during that period. When we use TDMA in a smart lab, any other node in its vicinity can hear the information that each node in its network sends.

To ensure optimal performance of an ANCC system, the channels connecting the nodes must be orthogonal using TDMA.

It is very important to develop a method that guarantees that all the nodes that share that medium can transmit the medical data without errors.

The motivation for using this multiplexing technique and no other is that our algorithm requires that all nodes be capable of transmitting and receiving health data from other nodes. TDMA is the simplest way to implement this critical application.

We present the ANCC using the NC scheme in this paper. This scheme seeks to match the snapshot subnet topology with the channel-coding graph.

The ANCC scheme's concept is that each node listens to health data communicated by its neighbors and then sends a portion of that data to the destination node.

This process is analogous to a distributed encoding channel. The network nodes build the generating matrix of an LDPC code because each node communicates with many packets: the packet that transmits the node's health data and the packet corresponding to the combination of the health data received from other nodes. These packets correspond to columns of the generating matrix G.

The parity check matrix H assists the destination node in decoding information from a group of decision nodes after the communication steps (sending each node and forwarding data outside each node) are completed.

This ANCC scheme will use LDGM (Low-Density Generator Matrix) codes for LDPC coding [53]. Their extremely simple coding characterizes the distributed coding of LDGM codes.

The identity matrix I_N is concatenated with a sparse matrix P, defined by the information that combines each node to generate the G in these codes. In these codes, the identity matrix I_N is concatenated with a sparse matrix P, defined by the information that combines each node to generate the G. When the t rate is 1/2, each information bit is preceded by another parity check.

The LDPC codes were specified as CLDPC codes (n, j, k), where n is the length of the code words, j is the number of ones in each column, and k is the number of ones in each row. An LDPC code's generating matrix G must be sparse. A sparse matrix [54] is a binary matrix in which most values are zeros. We assume that each HDA aggregates health data from multiple voluntary patients denoted $N_{i,j}$,$(i = 1, 2, .., mj = 1, 2 \ldots, n)$ of each subnet. The HDA node relative to each patient contains the medical information necessary to judge the evolution of the virus type analyzed. The ANCC plan is divided into the first, second, and coding stages. The second and third stages are composed of three distinct phases. In our case, an extremely sparse matrix will be $n \gg j, k$.

1) *The Diffusion phase*: Each node broadcasts its packet in the slot given during this phase. Along with said slot, the central node and the rest of the network nodes stay quiet, enabling them to receive and store the packet. At the same time, the network's nodes examine the conditions under the reception of each packet and the channel's state during each packet's receipt. This information could then be used during the forwarding phase;
2) *The forwarding phase*: Each subnet node transmits a linear combination of some packets from the other nodes in the previous phase to the CN. Each subnet node selects the e most precisely received packets from the information gathered during the dissemination phase and participates in the said combination, which consists of the binary sum of those packets. After obtaining the packet, each node sends it to the CN in its designated slot.
3) *The decoding phase*: After receiving all packets from the two preceding steps, the CN begins decoding the big medical data. The Sum-Product algorithm is used for this decoding.

B. AN OVERVIEW OF LDPC CODING

The coding of LDPC codes is no different from coding any block code. The vectors and matrices involved in the coding of our algorithm are summarized as follows.

Information vector u: is the vector composed of the N bits of information, each of them coming from each of the nodes transmitting the information:

$$u = [u_1, u_2, u_3, \ldots, u_N] \tag{3}$$

A matrix of size $N \times 2N$ is used to generate the coded words. This matrix is defined by the identity matrix I_N and the parity matrix P, which generates the parity bits in the coded words. The form of obtaining the P matrix depends on parity equations. In the next section, we will see how to obtain the P in the present context.

Generator matrix G is a matrix of size $N \times 2N$ used to generate the coded words. This matrix is defined by the identity matrix I_N and the matrix P, responsible for generating the parity bits in the coded words. The form to obtain the matrix P depends on the parity equations we want to use. The following section shows the first stage and how these parity equations can be obtained.

$$G = [I_N \times P] \tag{4}$$

Vector of encoded information c: The vector resulting from encoding the information vector u with the generator matrix G. It has a length of $2N$ so that the first N bits correspond to the original information bits, and the last N bits correspond to linear combinations (defined by the matrix P)

of the information bits.

$$c = u \times G = [c_1, c_2, \ldots, c_N, c_{N+1}, c_{N+2}, \ldots, c_{2N}] \quad (5)$$

with

$$[c_1, c_2, \ldots, c_N] = [u_1, u_2, \ldots, u_N] \quad (6)$$

and

$$[c_{N+1}, c_{N+2}, \ldots, c_{2N}] = [u_1, u_2, \ldots, u_N] \times P \quad (7)$$

The parity check matrix H is the matrix for the systemic code generated by G, with $N \times 2N$ dimensions.The matrix H is built so that the product of the row vectors of the matrix G and those of the matrix H are orthogonal.

$$H = [P^T, I_N] \quad (8)$$

$$G \times H^T = 0 \quad (9)$$

where P^T and H^T are the transposed matrices of P and H, respectively. Syndrome vector s results from checking a word with the parity check matrix H. When decoding by syndrome, it must be fulfilled that the syndrome of a valid coded word c must be the null vector, as follows:

$$s = c \times H^T \quad (10)$$

Substituting and applying (7) and (8), we obtain that:

$$s = u \times G \times H^T = u \times 0 = 0 \quad (11)$$

It is deduced that a vector x corresponds to a codeword if it is fulfilled that:

$$x \times H^T = 0 \quad (12)$$

To decode the LDPC codes generated in our algorithm, we will use the Sum-Product algorithm (SPA) defined in [55] to apply to ANCC. The SPA is an iterative algorithm that estimates the a posteriori probability of the packets from the parity check matrix, the received packets, and the likelihood of the packets traversing the channel.

C. INFLUENCE OF THE NUMBER OF NETWORK NODES

We demonstrate the need for LDPC codes to be generated by highly dispersed matrices; this characteristic favors the decoding process. The generator matrix G size is influenced by the number of nodes participating in the encoding. The G size for a given number of nodes, N, is $Ntimes2N$.

Thus, if the parameter's value is fixed, a greater number of nodes would cause a greater dispersion of the G since the ratio of non-null values concerning the total number of elements of the matrix will be smaller. We define the degree of dispersion DD as:

$$DD = \frac{e}{N-1} \quad (13)$$

The parameter "e" corresponds to the number of packets originating from the nodes that contribute to the response of each node during the forwarding phase. These packers must intervene in each node's response during the forwarding phase; N represents the total number of nodes in a specific group. This parameter, DD, represents the percentage of packets that interfere in the response during the forwarding phase from all packets that potentially intervene.

The goal is to see if you can get a range of DD values between which the algorithm behaves optimally to establish a priori the values of the parameter e and the number of nodes that give the best $BER - SNR$ curves.

IV. HIERARCHICAL ALGORITHM: FIRST STAGE

The first stage of the hierarchical algorithm focuses on the initial data collection process in healthcare. It emphasizes the importance of collecting big data to address various medical problems effectively. This stage strategically guides the decision-making process of a smart laboratory, enhancing healthcare facilities' visibility, effectiveness, and dependability through data aggregation. The principles of HDA and the Basic Conception form the foundation of this initial stage.

A. THE IMPORTANCE OF COLLECTING BIG DATA IN HEALTHCARE: THE FIRST STAGE OF THE ALGORITHM

Before receiving a vaccine, individuals should assess their overall health to understand its potential impact on the experimental results. Data aggregation is crucial in addressing various issues within the medical sector. It is vital for improving healthcare institutions' transparency, efficiency, and dependability. Collecting big data in healthcare serves as the crucial initial step in addressing various medical problems and serves as the foundation of our algorithm. This gathered information strategically guides the decision-making process of a smart laboratory. By aggregating data, healthcare facilities can enhance their visibility, effectiveness, and dependability. This initial stage is built upon the fundamental principles of the HAD and the Basic Conception. The interactions between patients and healthcare facilities in the industry result in valuable patient data, which is important in informed decision-making, enhancing treatment outcomes, and advancing medical research. Patient interactions with healthcare facilities lead to the creation of patient data, including their name, medical background, age, diagnosis, course of treatment, and family history. This data is essential for providing patients with the best possible care. Comprehensive patient knowledge, including medical history, diagnoses, treatments, and family background, empowers doctors to make better treatment decisions. Aggregated healthcare data expands this advantage by enabling the analysis of hundreds or thousands of similar cases. This broader perspective provides valuable insights, identifies patterns and trends, and guides optimal treatment approaches based on collective patient outcomes.

B. THE IMPACT OF DATA SHARING ON HEALTHCARE BUSINESS AND TREATMENT EFFICIENCY

Medical professionals may create more efficient treatments by combining the data of many comparable instances,

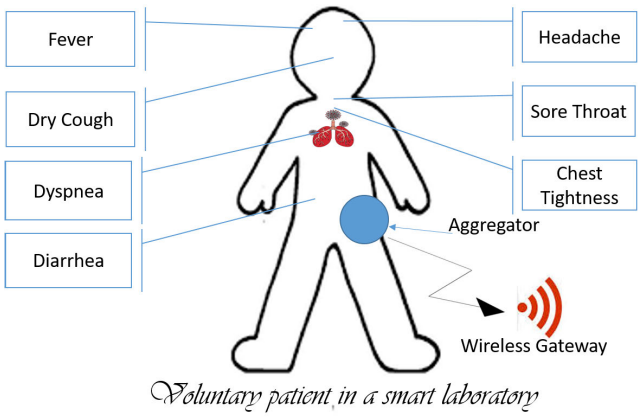

FIGURE 4. An overview of the node description system is given above. We think of each node as a patient who has received a certain type of vaccine, and we watch how the patient's condition changes through his *HDA*s.

speeding up healthcare delivery. The best use of data even has the potential to save thousands of lives. However, it's important to note that even if the combined data do not provide physicians with all the information they need to treat patients, they can still use it to plan strategically and improve healthcare systems. For collected data to result in evidence-based decision-making that benefits organizations, appropriate data aggregation technologies are required. Sharing healthcare data brings numerous benefits and significantly improves care for both payers and individuals who benefit from data aggregation in the healthcare industry. The integration of big data and AI in healthcare is now a subject that medical professionals and healthcare providers can explore to develop new strategies for improving the effectiveness of their therapies. We discuss several aspects demonstrating how data sharing affects healthcare, ultimately increasing our understanding of HDA.

C. THE CONCEPT OF A DENSE SMART LABORATORY AND ITS APPLICATION IN VIRUS SYMPTOM ANALYSIS

In our research, we explore the concept of a dense smart laboratory, which refers to a setting where numerous voluntary patients are located in a small area. Within this dense network, each node is within the coverage radius of several neighboring nodes, establishing interconnected neighborhoods. The smart laboratory is divided into m regular groups, or subnets, each containing n nodes and one CN, resulting in a total of m CNs. The medical information data we consider in this context primarily focuses on virus symptoms, specifically those related to COVID-19, such as fever, dry cough, dyspnea, diarrhea, headache, and sore throat, as illustrated in Fig 4.

Each node in this dense smart laboratory represents a patient's HDA, equipped with multiple medical sensors that provide doctors with information about the symptoms of the tested virus. To manage the flow of medical information, the patient's HDA nodes are partitioned into subnets, and each subnet consists of a CN that communicates with one or more RN. These subnet nodes serve as a source of medical information that reflects the ongoing analysis of the patient's viral status evolution.

V. HIERARCHICAL ALGORITHM: SECOND STAGE

The focus is on the CNs in the second hierarchical stage of the proposed algorithm. These CNs play a crucial role in performing several essential functions. Firstly, they collect measured data from the HDA nodes. Once collected, the CNs process and store the processed data in a central database. Additionally, they provide a means for displaying the status of the measuring system and the measured data to the operator.

A. GENERAL OVERVIEW OF THE SECOND STAGE

The CNs generate comprehensive reports on measurements conducted throughout the algorithm, ensuring a comprehensive overview of the data collected. To facilitate easy access and visualization, the collected data is presented using Web technology, making it accessible and user-friendly. The CNs serve as the central hub, orchestrating these functions and enabling effective data management and reporting within the algorithm.

Fig. 5 shows the second stage of the proposed algorithm of how the ANCC scheme uses NC with LDGM codes. We consider n used aggregators in each subnet, with e combining packets for the forwarding phase. Although LDGM codes are not being used in this second stage, the generating matrix must not be very dense, and it can illustrate quite clearly the steps that are followed in coding this type of code.

All the presented nodes in the smart laboratory reached their CNs in a single hop and wanted them to reach the RN again with only one hop. This scheme makes the analysis much easier and simpler, but this scheme is difficult to represent in another real environment. Several hops may also be difficult to represent in a real environment. Several hops may appear to reach the RN. This phenomenon depends, among other factors, on the number of nodes, the distance between them, and the technology used.

The number of hops required to reach the RN node in our critical application can vary based on several factors, including the number of nodes, the distance between them, and the network and technology used. Other factors can also come into play when determining the sufficiency of a single hop. For this reason, a hierarchical algorithm based on three stages is presented in this paper. The strategy divides all nodes into networks or groups that include many HDA nodes.

All patient HDA nodes of the same network are chosen to directly link to guarantee optimum system performance with the grouping's most important node (central node). On the other hand, all CNs are selected n again to link with the RN node directly. The element receives and decodes all the information of each patient grouping for multi-virus-specific prevention or treatment against the recent virus, including COVID-19. This node will be the destination

TABLE 1. Structure and composition of a subnet in a smart laboratory.

Group / subnet	HDA nodes of each group	Central node
1	$N_{1.1}$,$N_{1.2}$,...,$N_{1.n}$	N_1
2	$N_{2.1}$,$N_{2.2}$,...,$N_{2.n}$	N_2
⋮	⋮	⋮
m	$N_{m.1}$,$N_{m.2}$,...,$N_{m.n}$	N_m

node of the trans-missions made by the rest of the subnet nodes. The smart laboratory contains m subnets in our algorithm, each containing n aggregators' nodes. Consider subnet 1; it is composed of n HDA nodes labeled $N_{1.1}$, $N_{1.2}$, $N_{1.3}$,...,$N_{1.n}$, and a N_1, the RN. Each subnet has the same number of HDA nodes with the same functionality within the smart laboratory. Subnet 2 is composed of n nodes labeled $N_{2.1}$,$N_{2.2}$, $N_{2.3}$,...,$N_{2.n}$, and a N_2, the RNs, and so on as shown in the following Table 1.

where N_i,j are the efficient wireless body area network (WBAN) aggregators of the *ith* subnet of the *jth* patient, and the RN is the node that should receive all virus-type information, including the COVID-19 outbreak. Figs. 5(a, b, c, and d) show how the nodes store data in the diffusion phase. Consider group 1; the transmission of node $N_{1.1}$ is depicted in Fig. 5(a). Node $N_{1.1}$ transmits its packet $p_{1.1}$, and both the central node and the rest of the nodes remain silent and listen to the packet that node $N_{1.1}$ has transmitted. The remaining nodes analyze the received information and verify whether the packet is well received. If a node determines that a packet has been received correctly, it saves the packet delivered by node $N_{1.1}$. If this is not the case, the packet will be discarded.

The algorithm's data-receiving nodes are $N_{1.h_1}$ and $h_1 \leq n$. Furthermore, the CNs store the correctly received data packet from node $N_{1.1}$. Fig. 5 (b) depicts the transmission of node $N_{1.2}$. As with node $N_{1.1}$, node $N_{1.2}$ broadcasts its packet while the remaining HDA in subnet 1 listens to the channel and stores the packet $p_{1.2}$ if it is considered to have been received correctly. During this broadcast, different nodes $N_{1.h_1}$ of subnet 1 store the packet $p_{1.2}$

As illustrated in Fig.5, these processes are repeated for broadcasting the remaining packets $p_{1.3}$, $p_{1.4}$, ..., $p_{1.n}$ of the *HDA* nodes of the subnet 1 $N_{1.3}$, $N_{1.4}$...,$N_{1.n}$ (3). Finally, as seen in Fig.5 (4), we can observe the outcome of the broadcasting operation. Therefore, we have an HDA set that has participated in storing each of the correctly received packets. The CN has received all the packets $p_{1.1}$, $p_{1.2}$,..., $p_{1.n}$, while the other nodes belonging to subnet 1 can receive packets whose signal level exceeds the requested reception sensitivity Fig.6, detailed in Table 2.

As shown in Table 2, each node chooses the packets that have been correctly received in the previous phase. The results of the packets that each node has stored in the broadcasting phase are:

So the information vectors u_1, u_2,..., $u_{m)}$ made up of the packet of the network 1, 2, ..., m respectively, we, therefore, have the following Table 3:

TABLE 2. The packets that were received from the HDAs belong to subnet 1 in a smart laboratory.

Nodes of each subnet	packets received from nodes of subnet 1
N_1	$\sum_{j=1}^{n}(p_{1.j})$, $j \in \{1,2,\ldots,n\}$
$N_{1.1}$	$\sum_{j=1}^{h_{1.1}}(p_{1.j})$, $j \in \{1,2,\ldots,n\} \cap j \neq 1, h_{1.1} \leq n-1$
$N_{1.2}$	$\sum_{j=1}^{h_{1.2}}(p_{1.j})$, $j \in \{1,2,\ldots,n\} \cap j \neq 2, h_{1.2} \leq n-1$
$N_{1.3}$	$\sum_{j=1}^{h_{1.3}}(p_{1.j})$, $j \in \{1,2,\ldots,n\} \cap j \neq 3, h_{1.3} \leq n-1$
⋮	⋮
$N_{1.n}$	$\sum_{j=1}^{h_{1.n}}(p_{1.j})$, $j \in \{1,2,\ldots,n\} \cap j \neq n, h_{1.n} \leq n-1$

TABLE 3. Obtened packets from a variety of *HDA* operating inside their subnets in a smart laboratory.

information vector	packets received from various HDAs in their respective subnets
u_1	$p_{1.1}$,$p_{1.2}$, $p_{1.3}$,...,$p_{1.n}$
u_2	$p_{2.1}$,$p_{2.2}$, $p_{2.3}$,...,$p_{2.n}$
u_3	$p_{3.1}$,$p_{3.2}$, $p_{3.3}$,...,$p_{3.n}$
⋮	⋮
u_m	$p_{m.1}$,$p_{m.2}$, $p_{m.3}$,...,$p_{m.n}$

TABLE 4. Responses from the *HDA*s present in subnet1.

Nodes of each subnet	Responses	Subnet
$N_{1.1}$	$\sum_{j=1}^{e_{1.1}+1} \overset{e_{1.1}}{\oplus} p_{1.j}$, $j \in \{1,2,\ldots,n\} \cap j \neq 1$	Subnet1
$N_{1.2}$	$\sum_{j=1}^{e_{1.2}+1} \overset{e_{1.2}}{\oplus} p_{1.j}$, $j \in \{1,2,\ldots,n\} \cap j \neq 2$	
$N_{1.3}$	$\sum_{j=1}^{e_{1.3}+1} \overset{e_{1.3}}{\oplus} p_{1.j}$, $j \in \{1,2,\ldots,n\} \cap j \neq 3$	
⋮	⋮	
$N_{1.n}$	$\sum_{j=1}^{e_{1.m}+1} \overset{e_{1.m}}{\oplus} p_{1.j}$, $j \in \{1,2,\ldots,n\} \cap j \neq n$	

When all HDA nodes have transmitted their packets, the global information vector is:

$$u = \left[\underbrace{\sum_{j=1}^{n}(P_{1,j}) \quad \sum_{j=1}^{n}(P_{2,j}) \quad \sum_{j=1}^{n}(P_{3,j}) \ldots \sum_{j=1}^{n}(P_{m,j})}_{\textit{Native packets}} \right] \tag{14}$$

Once all nodes have transmitted their packet, the forwarding phase begins. In that case, each node will only send the packets that it has successfully received, leaving the generator matrix G with a number below the e_1, e_2,..., e_m, ones in the corresponding column where e is the number of coded packets (combined) and will be the same for all the networks of the smart laboratory. Each node has produced the following outputs responses as in Table 4:

where symbol $\oplus$ represents the binary sum of packets sent in the forwarding phase.

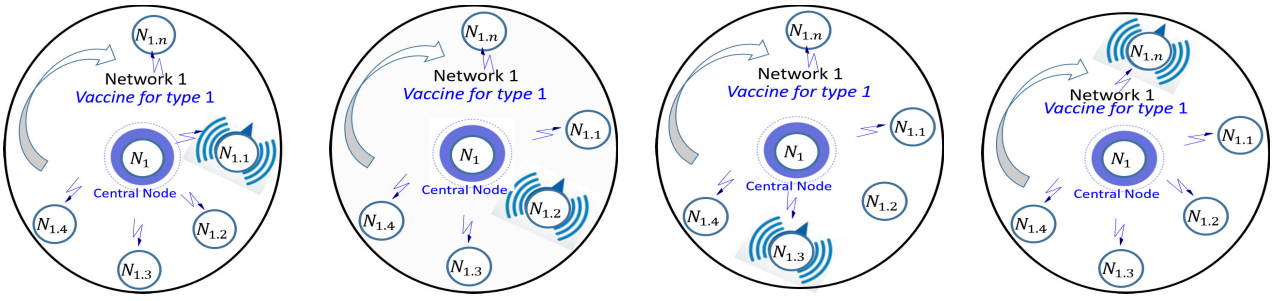

FIGURE 5. The second stage of the proposed algorithm of sending phase with n nodes. It's about a wireless communication scheme in a subnet 1. (a) Case $N_{1.1}$. (b) Case $N_{1.2}$. (c) Case $N_{1.3}$. (d) Case $N_{1.n}$.

Table 4 depicts the behavior of the forwarding phase nodes, which is quite similar to that of the nodes in the broadcast phase. Each node broadcasts the new packet elaborated on while the rest remain silent. The main difference between the two phases is that in this second phase, the nodes no longer need to listen to the packets transmitted by the other nodes. Only the CN node must listen to them and store the packets in this second phase. The process that corresponds to the forwarding phase is as follows:

First, all the nodes in each subnet prepare the packet to be sent in the forwarding phase. Therefore also that $e = e_{i.j}$, $i \in \{1, 2, \ldots, m\}$,$j \in \{1, 2, \ldots, n\}$. Subsequently, node $N_{1.1}$ sends the packet corresponding to $\sum_{j=1}^{e_{1.1}+1} \overset{e_{1.1}}{\oplus} p_{1.j}$ and with the necessary headers to decode it at the CN. The CN receives and stores the information received. Finally, the CN has received all the data corresponding to both phases. Thus, after these two phases, from equations (4) and (5), we have the vector of coded information c:

$$c = \left[\underbrace{\sum_{i=1}^{m}\sum_{j=1}^{n} P_{i.j}}_{\textit{Native packets}}, \underbrace{\sum_{i=1}^{m}\sum_{j=1}^{e} \overset{e}{\oplus} P_{i.j}}_{\textit{Coded packets}} \right] \tag{15}$$

These steps are repeated for nodes of subnet 1 transmitting their corresponding packets. Matrix P_1 is constructed from the information of the forwarding phase of subnet 1. From the previous data on the transmitting nodes and those, each node will combine in the forwarding phase, and the CN (N_1) can build the generator matrix G. The matrix that expresses the parity equations P_1 is needed. A column and a row represent each node in the network. Each column and row corresponds to each node that makes up subnet 1.

At this step, the matrix G_1 can be created using equation (2), and the obtained matrix P_1. In addition, from the matrix P, the CN can construct the parity check matrix H, as shown in equation (6).

The SPA will use this parity-check matrix H to obtain the transmitted u information vector.

As well as for all of the other types of vaccinations, we are following in the footsteps of $N_{1.1}$, $\sum_{j=1}^{n} N_{i\neq 1.j}$, $j \in \{1, 2, \ldots, n\}$,$i \in \{1, 2, \ldots, m\}$ proceed in the same way as for the $N_{1.1}$. We proceed the same way for the remaining subnets, basing and inspiring on the data of subnet 1, as shown in Tables 5 and 6.

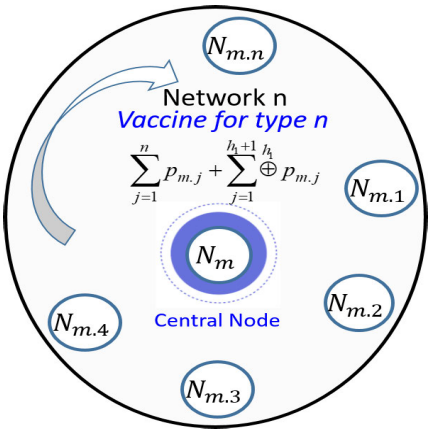

FIGURE 6. Overview of the node description scheme. Each node is considered a patient vaccinated with one type of vaccine, and we follow the signs of its evolution.

Fig.7 shows data information exchange over the smart laboratory's complete network.

As we have already illustrated for subnet 1, the medical data from the forwarding phase of each network are used to create the corresponding matrix, P_2,P_3,. . .,P_m. The central nodes can construct the generators matrix G_2, G_3,. . .,G_m from the primary data on the transmitting nodes and each node's data in the forwarding phase.

B. STUDY EXAMPLE FOR THE SECOND STAGE

We assume that we have only one group (subnet1) composed of six HDAs providing $p_{1.1}$, $p_{1.2}$, $p_{1.3}$, $p_{1.4}$, $p_{1.5}$, $p_{1.6}$ with one N_1 Fig.8 shows the composition of the second stage in subnet 1, using the proposed algorithm with 6 HDAs.

We still assume that:

$$u_1 = (p_{1.1}, p_{1.2}, p_{1.3}, p_{1.4}, p_{1.5}, p_{1.6})$$

TABLE 5. Packets are received from the aggregator nodes of each subnet.

CN and HDA of each subnet	packets received from nodes of subnets
	subnet 2
$N_2(CN)$	$\sum_{j=1}^{n} p_{2.j},\ j \in \{1,2,\ldots,n\}$
$N_{2.1}$	$\sum_{j=1}^{e_{2.1}}(p_{2.j}),\ j \in \{1,2,\ldots,n\} \cap j \neq 1, e_{2.1} \leq n-1$
$N_{2.2}$	$\sum_{j=1}^{e_{2.2}}(p_{2.j}),\ j \in \{1,2,\ldots,n\} \cap j \neq 1, e_{2.2} \leq n-1$
$\vdots$	$\vdots$
$N_{2.n}$	$\sum_{j=1}^{e_{2.n}}(p_{2.j}),\ j \in \{1,2,\ldots,n\} \cap j \neq 1, e_{2.n} \leq n-1$
$\vdots$	$\vdots$
	subnet m
$N_m(CN)$	$\sum_{j=1}^{n} p_{m.j},\ j \in \{1,2,\ldots,n\}$
$N_{m.1}$	$\sum_{j=1}^{e_{m.1}}(p_{2.j}),\ j \in \{1,2,\ldots,n\} \cap j \neq 1, e_{m.1} \leq n-1$
$N_{m.2}$	$\sum_{j=1}^{e_{m.2}}(p_{2.j}),\ j \in \{1,2,\ldots,n\} \cap j \neq 1, e_{m.2} \leq n-1$
$\vdots$	$\vdots$
$N_{m.n}$	$\sum_{j=1}^{e_{m.n}}(p_{2.j}),\ j \in \{1,2,\ldots,n\} \cap j \neq 1, e_{m.n} \leq n-1$

TABLE 6. Transmission number of the coded packets.

Nodes of each subnet	Reponses
$N_{2.1}$	$\sum_{j=1}^{e_{2.1}+1} \overset{e_{2.1}}{\oplus} p_{2.j},\ j \in \{1,2,\ldots,n\} \cap j \neq 1$
$N_{2.2}$	$\sum_{j=1}^{e_{2.2}+1} \overset{e_{2.2}}{\oplus} p_{2.j},\ j \in \{1,2,\ldots,n\} \cap j \neq 2$
$\vdots$	$\vdots$
$N_{2.n}$	$\sum_{j=1}^{e_{2.n}+1} \overset{e_{2.n}}{\oplus} p_{2.j},\ j \in \{1,2,\ldots,n\} \cap j \neq n$
$\vdots$	$\vdots$
$N_{m.1}$	$\sum_{j=1}^{e_{m.1}+1} \overset{e_{m.1}}{\oplus} p_{m.j},\ j \in \{1,2,\ldots,n\} \cap j \neq 1$
$N_{m.2}$	$\sum_{j=1}^{e_{m.2}+1} \overset{e_{m.2}}{\oplus} p_{m.j},\ j \in \{1,2,\ldots,n\} \cap j \neq 2$
$\vdots$	$\vdots$
$N_{m.n}$	$\sum_{j=1}^{e_{m.n}+1} \overset{e_{m.n}}{\oplus} p_{m.j},\ j \in \{1,2,\ldots,n\} \cap j \neq n$

Thus, based on our example and equations (4) and (5), the resultant coded information vector c is as follows (16), shown at the bottom of the next page.

A packet $p_{i.j}$ has a value of 1 if the node corresponding to row i participates in the binary sum of the response corresponding to column j, 0 if it does not participate. With this, the resulting matrix P_1 for the previous example is:

$$P_1 = \begin{bmatrix} N_{1.1} & N_{1.2} & N_{1.3} & N_{1.4} & N_{1.5} & N_{1.6} & \\ 0 & 1 & 0 & 1 & 0 & 0 & N_{1.1} \\ 1 & 0 & 0 & 0 & 1 & 0 & N_{1.2} \\ 0 & 0 & 1 & 0 & 0 & 1 & N_{1.3} \\ 0 & 1 & 0 & 0 & 1 & 0 & N_{1.4} \\ 0 & 0 & 1 & 0 & 0 & 1 & N_{1.5} \\ 1 & 0 & 0 & 1 & 0 & 0 & N_{1.6} \end{bmatrix} \tag{17}$$

In the upper part, the nodes correspond to columns; in the right part, the nodes correspond to the rows. Thus, for example, a 1 is the value of the element corresponding to row $N_{1.2}$ and column $N_{1.1}$ if the packet transmitted by node $N_{1.1}$ in the forwarding phase carries information of the packet transmitted by node $N_{1.2}$, as it happens in this case.

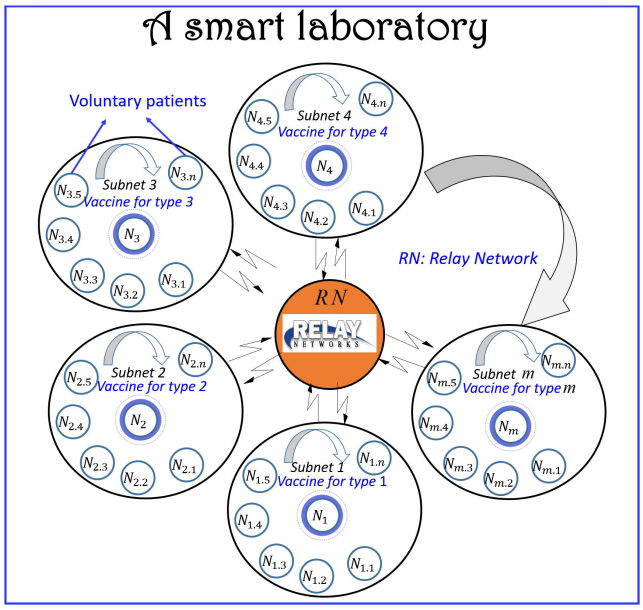

FIGURE 7. The information is exchanged between HDAs and the CNs on the one hand, and they are exchanged between CNs via RN on the other hand. Each HDA is considered a patient inoculated with a specific vaccine, and we monitor its progress.

The matrix G_1 that generates this code may be constructed using equation (2) and the matrix P_1:

$$G_1 = \begin{bmatrix} 1 & 0 & 0 & 0 & 0 & 0 & 0 & 1 & 0 & 1 & 0 & 0 \\ 0 & 1 & 0 & 0 & 0 & 0 & 1 & 0 & 0 & 0 & 1 & 0 \\ 0 & 0 & 1 & 0 & 0 & 0 & 0 & 0 & 1 & 0 & 0 & 1 \\ 0 & 0 & 0 & 1 & 0 & 0 & 0 & 1 & 0 & 0 & 1 & 0 \\ 0 & 0 & 0 & 0 & 1 & 0 & 0 & 0 & 1 & 0 & 0 & 1 \\ 0 & 0 & 0 & 0 & 0 & 1 & 1 & 0 & 0 & 1 & 0 & 1 \end{bmatrix} \tag{18}$$

In addition, the CN node can construct the matrix H from the matrix P, as given in equation (6):

$$H_1 = \begin{bmatrix} 0 & 1 & 0 & 0 & 0 & 1 & 1 & 0 & 0 & 0 & 0 & 0 \\ 1 & 0 & 0 & 1 & 0 & 0 & 0 & 1 & 0 & 0 & 0 & 0 \\ 0 & 0 & 1 & 0 & 1 & 0 & 0 & 0 & 1 & 0 & 0 & 0 \\ 1 & 0 & 0 & 0 & 0 & 1 & 0 & 0 & 0 & 1 & 0 & 0 \\ 0 & 1 & 0 & 1 & 0 & 0 & 0 & 0 & 0 & 0 & 1 & 0 \\ 0 & 0 & 1 & 0 & 1 & 0 & 0 & 0 & 0 & 0 & 0 & 1 \end{bmatrix} \tag{19}$$

The SPA will use this parity check matrix H_1 to obtain the information vector u_1 transmitted.

VI. HIERARCHICAL ALGORITHM: THIRD STAGE

The previous section introduced the ANCC algorithm, which utilizes NC with LDPC in the second stage. Building upon that, this section focuses on the third stage of the ANCC scheme, which involves the subnets with RN. These subnets play a crucial role in the ANCC scheme presented earlier, and their significance will be explored in further detail.

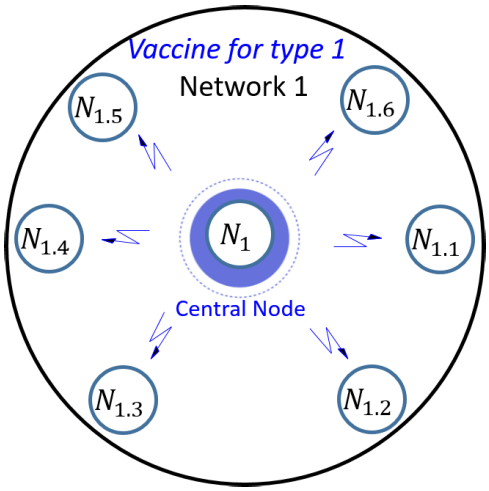

FIGURE 8. The second stage uses the proposed algorithm with 6 HDAs exchanging information in the wireless communication scheme in subnet 1 via the central node N_1.

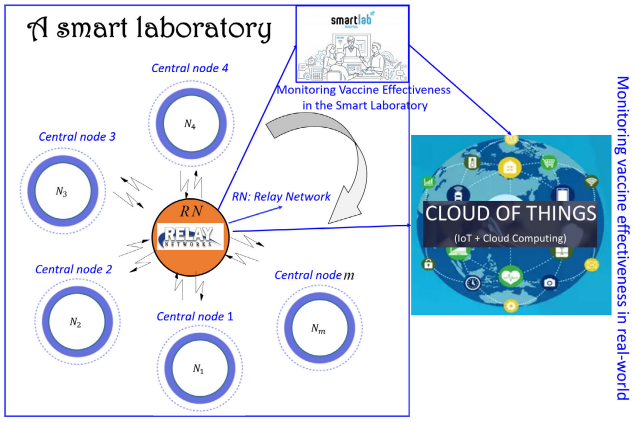

FIGURE 9. An overview of the proposed scheme The smart laboratory consists of ($n \times m$) HDAs and m subnets.

A. GENERAL OVERVIEW OF THE THIRD STAGE

The relay subnets' nodes form the third stage, which sends all the information from their aggregator to the CNs.

Since the second level has a very small number of central nodes, we will obtain generator matrices that cannot be very dispersed if the same scheme is used directly in the previous level; the ANCC scheme, at this point, does not offer good results. To guarantee the good behavior of our algorithm, we propose, for the second level, to modify the generator's matrix so that each CN sends all the packets received from its subnets. In addition, all of them must participate in constructing the G as independent elements. This idea is considered because their contributions to the G are independent, even if all packets come from the same node. To investigate how the channel is affected, we use the coherence time (T_c), defined as the time when a channel remains roughly constant. The corresponding G will have a few linearly independent columns if the coherence time is very high. At this third stage, since we have a few CNs containing big data, the channels cannot be guaranteed to vary between transmissions of several consecutive packets. For this reason, coherence time plays a fundamental role when designing the generator matrix. The proposed algorithm tries to give each channel independence, and the coherence time can't be changed; burst transmission is the best way to describe fast transmission.

A burst is the set of packets that each node transmits consecutively. When a burst includes β transmitted packets, its duration is T_β, where β is the number of packets per burst. The HDA nodes take turns transmitting either one.

If k nodes are involved, the coherence time T_c is less than $k \times T_\beta$ and, therefore, the next time is the turn of the same node to transmit, the channel will have changed, offering data on a different channel from the previous burst.

Practically, we want to ensure the coherence time has the shortest possible duration. So that each burst encompasses very few packets so that the number of packets correlated by the same channel is as small as possible. Therefore, the columns of the code G will be more independent.

In this way, the size of the bursts must be such that the following equation is satisfied:

$$T_\beta \geq \frac{T_c}{m} \tag{20}$$

where m represents the central nodes number involved, T_β, is the burst duration, and T_c is the channel coherence time. Substituting the expression to find the burst size duration into equation (20), we have that:

$$\beta \geq \frac{T_c}{m \times T_s} \tag{21}$$

We note that $\alpha = \frac{n}{\beta}$ is the number of bursts per node of each network, the β is the number of packets per burst, and T_s is the time taken to transmit one packet. We suggest the following steps to understand how nodes work at this second stage. We suppose that we have a total of $n \times m$ *HDA*s at the first stage and, therefore, m CNs that will transmit information to an RN. The RN includes a total of m CNs, and then we have the following scheme Fig.9.

All *CNs* ($N_1, N_2, \ldots, N_m$) have correctly received all native packets, and many coded packets coming from the patient HDAs, and each CN wants to send its packets as shown in Table 7.

$$c = \Big[\underbrace{p_{1.1}, p_{1.2}, p_{1.3}, p_{1.4}, p_{1.5}, p_{1.6}}_{\textit{Native}\text{ packets}}, \underbrace{p_{1.2}\oplus, p_{1.6},\ p_{1.1}\oplus,\ p_{1.4}, p_{1.3}\oplus, p_{1.5},\ p_{1.1}\oplus, p_{1.6},\ p_{1.2}\oplus, p_{1.4},\ p_{1.3}\oplus, p_{1.5}}_{\textit{Coded}\text{ packets}}\Big] \tag{16}$$

TABLE 7. Transmission number of the native packets.

CN of each subnet	packets transmitted from HDA of subnets, as in Table 6
N_1 is the CN of subnet 1	Transmission of the informations from $N_{1.1}$, $N_{1.2}$, . . ., $N_{1.n}$
N_2 is the CN of subnet 2	Transmission of the informations from $N_{2.1}$, $N_{2.2}$, . . ., $N_{2.n}$
N_3 s the CN of subnet 3	Transmission of the informations from $N_{3.1}$, $N_{3.2}$, . . ., $N_{3.n}$
⋮	⋮
N_m s the CN of subnet m	Transmission of the informations from $N_{m.1}$, $N_{m.2}$,. . ., $N_{m.n}$

We suppose each CN transmits bursts of β packets and the coherence time T_c below $m.\beta.T_p$. After the m CNs nodes transmit their burst, it can be considered that the channel has varied since the equation is fulfilled (21). If this equation is not fulfilled, the nodes should transmit bursts with a greater number of packets per burst to guarantee the variability of the channel. The steps to be followed in this transmission are listed below in order:

Node N_1 begins the transmission of a burst with the first β_1^1 packets coming from its N_1: β_1^1=p_1^1,p_2^2,. . .,p_β^1, where β_i^j is the burst of the *ith* packet of the *CN* of the *jth* network. The rest of the network CNs keep silent, listening to the transmission of node N_1 and storing β packets, where $\beta \leq \beta_1^1$ packets if it has received them correctly. In turn, the CN nodes store packets.

After node N_1, node N_2 transmits the first β_1^2 packets: β_1^2=p_1^2,p_2^2,. . .,p_β^2.The RN node stores packets, and the rest of the CNs network listens and stores the packets if received correctly.

This same step is repeated for the rest of the *CN* network, nodes N_3,N_4,N_5,. . .,N_m, transmitting their first packets: β_1^3,β_1^4,β_1^5,. . ., β_1^m, respectively. Once the last node of the smart laboratory networks has transmitted its first packets, the N_1 transmits the next $\beta^1_{\beta_1^1+1}$ packets, which are: $\beta^1_{\beta_1^1+1}$=$p^2_{\beta_1^1+1}$,$p^1_{\beta_1^1+2}$,. . .,$p^1_{2\beta_1^1}$. The RN node stores the received data, and the rest of the CNs listen and store the packets if received correctly. Since the time elapsed since the transmission of N_1 started complies with equation (21), it is understood that the channel has changed. In the same way, all the CNs transmit again until they have transmitted all their packets. At that moment, the RN will receive all the packets from the smart laboratory, CNs, and RN. Consequently, these nodes will have enough information about describing a patient's health status to elaborate a response in the forwarding phase.

We presume that Table 8 summarizes the rest of the network nodes' information integrated within the appropriately received packets.

Once all the packets have been sent correctly, the resending phase begins. Let us assume now that the value of the parameter e for our algorithm is $e = 3$, i.e.,

Each response sent in the forwarding phase is the binary sum of three packets received. Each node (N_1, N_2, N_3, . . ., N_m) is responsible for developing four responses, one for each packet received by each *CN* within its grouping.

Three correctly received packets are chosen randomly to determine the response for each combined packet.

TABLE 8. Transmission number of the native packets.

Node	Best packets heard
N_1	β_1^2
N_2	β_1^2
N_3	β_1^2
⋮	⋮
N_m	β_1^2

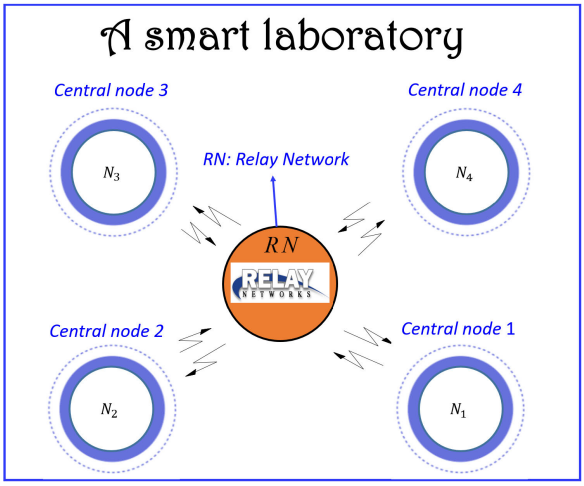

FIGURE 10. The proposed example scheme consists of 4 CNs relayed by one RN.

B. STUDY EXAMPLE FOR THE THIRD STAGE

To understand more clearly the operation of the nodes at this third stage, we propose the following example. Suppose four CNs have collected all the necessary information from the corresponding HDAs. There are four subnets; the CNs will transmit data to the RNs, as shown in Fig.10.

We have then the following scheme:

- The N_1, is the CN of subnet 1. It transmits the information that the *HDA*s are gathering from $N_{1.1}$, $N_{1.2}$, $N_{1.3}$, $N_{1.4}$, $N_{1.5}$, and $N_{1.6}$, received during the second stage which are denoted by $p^c_{1.1}$, $p^c_{1.2}$, $p^c_{1.3}$, $p^c_{1.4}$, $p^c_{1.5}$,and $p^c_{1.6}$, respectively.
- The N_2, is the CN of subnet 2. It transmits the data collecting by *HDA*s nodes from $N_{2.1}$, $N_{2.2}$, $N_{2.3}$, $N_{2.4}$, $N_{2.5}$, and $N_{2.6}$, received during the second stage which are denoted by $p^c_{2.1}$, $p^c_{2.2}$, $p^c_{2.3}$, $p^c_{2.4}$, $p^c_{2.5}$,and $p^c_{2.6}$, respectively.
- The N_3, is the CN of the subnet 3. It transmits the data collecting by *HDA*s from $N_{3.1}$, $N_{3.2}$, $N_{3.3}$, $N_{3.4}$, $N_{3.5}$,, and $N_{3.6}$, received during the second stage which are denoted by $p^c_{3.1}$, $p^c_{3.2}$, $p^c_{3.3}$, $p^c_{3.4}$, $p^c_{3.5}$,and $p^c_{3.6}$, respectively.
- The N_4, is the CN of subnet 4. It transmits the data collecting by *HDA*s from $N_{4.1}$, $N_{4.2}$, $N_{4.3}$, $N_{4.4}$, $N_{4.5}$, and

TABLE 9. Example of packets correctly received on the third stage.

Node	Best packets heard
N_1	$p^c_{1.1}$, $p^c_{1.2}$, $p^c_{1.3}$, $p^c_{1.4}$, $p^c_{1.5}$,and $p_{1.6}$
N_2	$p^c_{2.1}$, $p^c_{2.2}$, $p^c_{2.3}$, $p^c_{2.4}$, $p^c_{2.5}$,and $p^c_{2.6}$
N_3	$p^c_{3.1}$, $p^c_{3.2}$, $p^c_{3.3}$, $p^c_{3.4}$, $p^c_{3.5}$,and $p^c_{3.6}$
N_4	$p^c_{4.1}$, $p^c_{4.2}$, $p^c_{4.3}$, $p^c_{4.4}$, $p^c_{4.5}$,and $p^c_{4.6}$

$N_{4.6}$, received during the second stage which are denoted by $p^c_{4.1}$, $p^c_{4.2}$, $p^c_{4.3}$, $p^c_{4.4}$, $p^c_{4.5}$,and $p^c_{4.6}$, respectively.

Suppose that each node transmits bursts of two packets and that the coherence time is below $8 \times T_s$ so that after all four central nodes transmit their burst, the channel can be considered varied since equation (21) is satisfied. If this equation is not satisfied, the nodes should transmit bursts with more packets per burst to guarantee the channel's variability. The steps involved in this transmission are detailed in an orderly fashion below:

- The N_1 starts transmitting a burst with its two packets coming from its subnet: $p^c_{1.1}$ and $p^c_{1.2}$. The rest remain silent, listening to N_1 transmission and storing both packets if received correctly. In turn, the *RN* stores both packets.
- After the N_1, The N_2 transmits its first two packets coming from its subnet:$p^c_{2.1}$, $p^c_{2.2}$. The *CN* stores both packets; the rest listen and store the packets if received correctly.
- This same step is repeated for the rest of the *CN*s. The N_3, and N_4 transmit their first two packets: $p^c_{3.1}$, $p^c_{3.2}$ and $p^c_{4.1}$, $p^c_{4.2}$, respectively.
- Once the last CN node N_4 of subnet 4 has transmitted its first two packets, the N_1 of subnet 1 begins transmitting again the next two packets, which are packets $p_{1.3}$ and $p_{1.4}$. The RN stores the received data while the rest of the CNs listen and store packets that have been appropriately received. After the final node sends its initial symbols, the first node, N_1, transmits again. The channel has changed because the time since node N_1 commenced broadcasting (8 Ts) satisfies equation (21).
- In the same way, all the *CN*s of the smart laboratory transmit again until they have transmitted all their packets.

  At that time, all packets have been successfully transmitted. Therefore, the RN will receive all the packets from the CNs, so we have all the information necessary to elaborate global responses relative to each patient.

The assumed information gathered by the rest of the subnet HDAs is summarized in Table 9.

Suppose that the parameter e equals 3, i.e., each response sent in the forwarding phase is the binary sum of three received packets. Each $(N_1, N_2, N_3, andN_4)$ is required to provide four responses, one for each packet received by each HDA within its subnet. The answer for packets is generated by randomly selecting three well-received packets. Thus, an example of the possible responses elaborated by each CN associated with each packet could be those shown in Table 10.

TABLE 10. Formation of the parity matrix P for the third stage.

Node	Best packets heard
$N^c_{1.1}$	$p^c_{2.2} \oplus p^c_{3.3} \oplus p^c_{4.5}$
$N^c_{1.2}$	$p^c_{3.2} \oplus p^c_{4.3} \oplus p^c_{2.6}$
$N^c_{2.1}$	$p^c_{1.1} \oplus p^c_{1.4} \oplus p^c_{1.5}$
$N^c_{2.2}$	$p^c_{3.1} \oplus p^c_{4.2} \oplus p^c_{3.6}$
$N^c_{3.1}$	$p^c_{1.2} \oplus p^c_{2.3} \oplus p^c_{2.5}$
$N^c_{3.2}$	$p^c_{4.1} \oplus p^c_{4.4} \oplus p^c_{4.6}$
$N^c_{4.1}$	$p^c_{2.2} \oplus p^c_{1.3} \oplus p^c_{2.6}$
$N^c_{4.2}$	$p^c_{1.2} \oplus p^c_{1.5} \oplus p^c_{3.6}$
$N^c_{1.3}$	$p^c_{3.1} \oplus p^c_{2.3} \oplus p^c_{2.5}$
$N^c_{1.4}$	$p^c_{4.4} \oplus p^c_{3.5} \oplus p^c_{4.6}$
$N^c_{2.3}$	$p^c_{1.1} \oplus p^c_{3.2} \oplus p^c_{4.4}$
$N^c_{2.4}$	$p^c_{4.2} \oplus p^c_{3.3} \oplus p^c_{3.6}$
$N^c_{3.3}$	$p^c_{1.2} \oplus p^c_{1.4} \oplus p^c_{1.6}$
$N^c_{3.4}$	$p^c_{2.2} \oplus p^c_{4.3} \oplus p^c_{4.5}$
$N^c_{4.3}$	$p^c_{1.1} \oplus p^c_{2.3} \oplus p^c_{1.6}$
$N_{4.4}$	$p^c_{2.2} \oplus p^c_{1.3} \oplus p_{3.6}$
$N^c_{1.5}$	$p^c_{3.2} \oplus p^c_{1.3} \oplus p^c_{4.6}$
$N^c_{1.6}$	$p^c_{2.1} \oplus p^c_{4.2} \oplus p^c_{2.5}$
$N^c_{2.5}$	$p^c_{1.1} \oplus p^c_{4.3} \oplus p^c_{3.6}$
$N^c_{2.6}$	$p^c_{3.2} \oplus p^c_{1.5} \oplus p^c_{4.6}$
$N^c_{3.5}$	$p^c_{1.2} \oplus p^c_{1.4} \oplus p^c_{2.6}$
$N^c_{3.6}$	$p^c_{2.2} \oplus p^c_{2.4} \oplus p^c_{1.6}$
$N^c_{4.5}$	$p^c_{1.1} \oplus p^c_{3.4} \oplus p^c_{3.6}$
$N^c_{4.6}$	$p^c_{2.1} \oplus p^c_{2.3} \oplus p^c_{2.5}$,

From Table 10, we can construct the parity matrix. Thus, the matrix P is as follows:

At the same time, the columns correspond to each response sent in the forwarding phase. In this way, if the element that corresponds to column $N^c_{1.1}$ and row $p_{2.2}$ is a 1 (where the value 1 is framed in matrix (22)), as shown at the bottom of the next page, it means that in the first response sent by the CN of subnet 2, the packet $p_{2.2}$ intervenes.

After constructing the parity matrix P, the G and the H are produced in the same manner as the third stage, using equations (4) and (8). Using this example, we discover that we have dispersed the matrix with the greatest number of zeros. To further enhance the quality of the information obtained in the second and third stages, a distributed channel coding approach that combines NC and LDPC must be implemented.

VII. RESULTS AND ANALYSIS

This section analyzes the results based on a hierarchy PHA using NC with LDPC codes to reduce the BER in an extensive and dense Healthcare Wireless Network. The MATLAB simulation tool was utilized to recreate scenarios in which various parameters were modified. The results were then analyzed by studying the BER vs. SNR curve to observe the impact of these changes on the curve. The evaluation method for determining the superiority of a scenario involved inspecting its BER versus SNR curves and selecting the one that achieved a better trade-off between the BER values obtained at high and low SNR values. The BER-SNR curve for an LDPC code exhibits a distinctive pattern, which can be divided into three regions, similar to [56] and [57]. The first region corresponds to low SNR values, where the BER-SNR curve shows a gradual decline with a small slope until it

reaches a specific threshold. In this region, utilizing LDPC encoding results in higher BER levels than not using it. The second region, known as the Waterfall region, is characterized by a steep slope in the BER-SNR curve until it reaches a new threshold. After crossing this threshold, the slope decreases. The third region, the Error Floor, emerges at high SNR values. This region is characterized by a slope similar to the first region.

A. FIRST STAGE: HDA NODES DISPERSION DEGREE AND ITS INFLUENCE ON THE PHA

Suppose we define the total number of HDA nodes in the smart laboratory as N_{HDA} and divide them into regular groupings with the same number of nodes of each subnet N_g. In that case, we can get the number of central nodes N_{CN}:

$$N_{CN} = \frac{N_{HDA}}{N_g} \tag{23}$$

We utilize 1000 HDA nodes for our simulations as the overall number of nodes. The number of nodes per subnet in the third stage and the number of nodes per CN in the second stage depend on the total number of nodes employed.

Fig.11 shows the curves obtained in the simulations for the case of the fixed value of the parameters $e = 3, 4, 5, 6, 7, 8, 9, 10, 11, and\ 12$. We use sets of nodes of different sizes to carry out the simulations with sets of 100, 200, 300, . . . , 1000 *HDA*s. They are exact numbers into which the set of total central nodes can be divided, which causes there to be between 1 and 30 groups in the third stage.

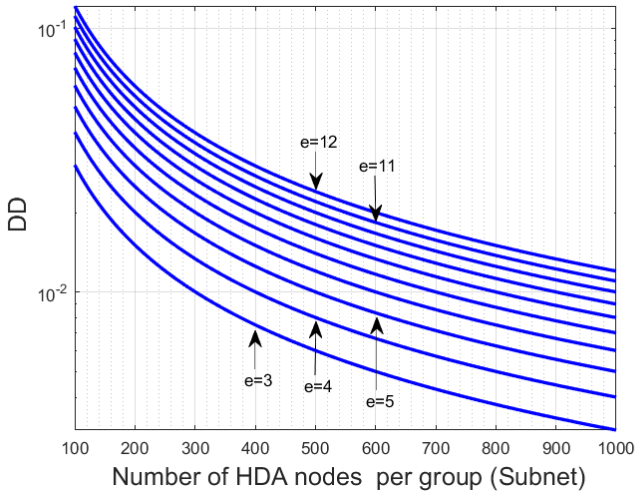

FIGURE 11. The relationship between the dispersion degree and the number of *HDAs* to illustrate the change in the parameter *e*.

Based on the findings of this study, it can be stated that the best degree of dispersion values depends on the number of nodes in the network.

B. SECOND STAGE: BETTER OPTION

Several simulations were run for nodes 100, 200, 300, and 400, with the following parameters: 3, 4, 5,... 12. The curves represented in Fig. 11 offer a better compromise for each HAD node of the study of the second stage. We compared

$$P = \begin{bmatrix}
0&0&1&0&0&0&0&0&0&0&1&0&0&0&1&0&0&0&1&0&0&0&1&0\\
0&0&0&0&1&0&0&1&0&0&0&0&1&0&0&0&0&0&0&0&1&0&0&0\\
0&0&0&0&0&0&0&0&0&0&0&0&0&0&0&0&1&0&0&0&0&0&0&1\\
\boxed{1}&0&0&0&0&0&1&0&0&0&0&0&0&1&0&1&0&0&0&0&0&1&0&0\\
0&0&0&1&0&0&0&0&1&0&0&0&0&0&0&0&0&0&0&0&0&0&0&0\\
0&1&0&0&0&0&0&0&0&0&1&0&0&0&0&0&1&0&0&1&0&0&0&0\\
0&0&0&0&0&1&0&0&0&0&0&0&0&0&0&0&0&0&0&0&0&0&0&0\\
0&0&0&1&0&0&0&0&0&1&0&1&0&0&0&0&0&1&0&0&0&0&0&0\\
0&0&0&0&0&0&1&0&0&0&0&0&0&0&0&1&0&0&0&0&0&0&0&0\\
0&0&1&0&0&0&0&0&0&0&0&0&1&0&0&0&0&0&0&0&1&0&0&0\\
0&0&0&0&1&0&0&0&1&0&0&0&0&0&1&0&0&0&0&0&0&0&0&1\\
0&0&0&0&0&0&0&0&0&0&0&0&0&0&0&0&0&0&0&0&0&1&0&0\\
1&0&0&0&0&0&0&0&0&0&0&1&0&0&0&0&1&0&0&0&0&0&0&0\\
0&0&0&0&0&0&0&0&0&0&0&0&0&0&0&0&0&0&0&0&0&0&1&0\\
0&1&0&0&0&0&0&0&0&0&0&0&0&1&0&0&0&0&1&0&0&0&0&0\\
0&0&0&0&0&1&0&0&0&0&1&0&0&0&0&0&0&0&0&0&0&0&0&0\\
0&0&1&0&0&0&0&1&0&0&0&0&0&0&0&0&0&0&0&1&0&0&0&0\\
0&0&0&0&0&0&0&0&0&0&0&0&1&0&0&0&0&0&0&0&1&0&0&0\\
0&0&0&0&1&0&0&0&1&0&0&0&0&0&0&0&0&1&0&0&0&0&0&1\\
0&1&0&0&0&0&1&0&0&0&0&0&0&0&1&0&0&0&0&0&1&0&0&0\\
0&0&0&0&0&0&0&0&0&1&0&0&0&0&0&0&0&0&0&0&0&0&0&0\\
0&0&0&1&0&0&0&1&0&0&0&1&0&0&0&1&0&0&1&0&0&0&1&0\\
1&0&0&0&0&0&0&0&0&0&0&0&0&1&0&0&0&0&0&0&0&0&0&0\\
0&0&0&0&0&1&0&0&0&1&0&0&0&0&0&0&1&0&0&1&0&0&0&0
\end{bmatrix} \tag{22}$$

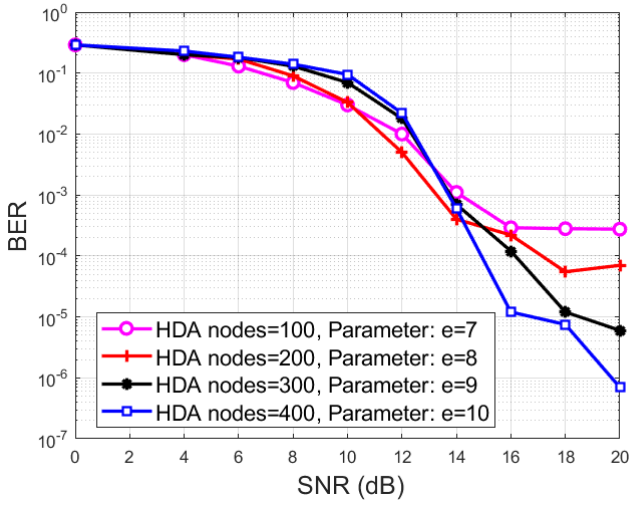

FIGURE 12. A comparison of the BER-SNR curves produced for a distributed LDPC encoding (the second stage of the technique that was provided) and those that offer a better compromise was carried out. The decoding method may go through a maximum of 10 iterations on each curve, and it compares groups of $HDA = 100$ with $e = 7$, $HDA = 200$ with $e = 8$, $HDA = 300$ with $e = 9$, and $HDA = 400$ with $e = 10$.

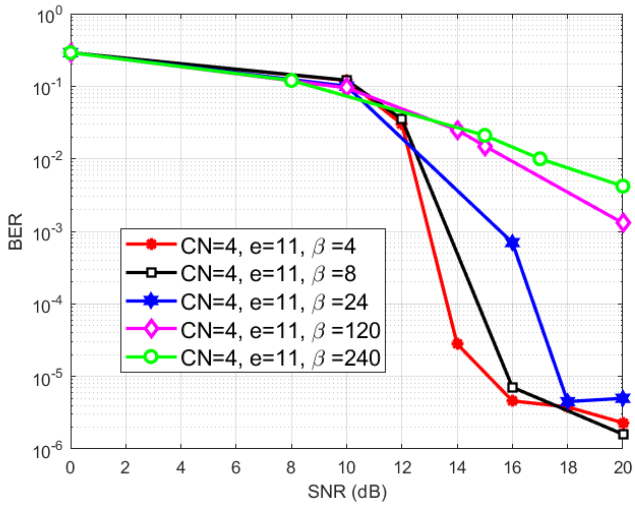

FIGURE 13. The BER-SNR curve was obtained for distributed LDPC coding (the third stage of the proposed algorithm) in a smart lab of 1200 HDAs, with 4 CNs and parameter value $e = 11$. The decoding algorithm can only be run ten times, and the value of β is 4,8,24,120,240, and e is 11.

TABLE 11. DD for the best curves of the second stage.

Number of HAD Node	Parameter e	DD
100	7	7.07%
200	8	4.52%
300	9	3.34%
400	10	2.2%

the groups of 100 HAD nodes (parameter e = 7), 200 HAD nodes (parameter e = 8), 300 HAD nodes (parameter $e = 9$), and 400 HAD nodes (parameter $e = 10$). The maximum number of iterations of the decoding algorithm for all curves is 10.

The curves shown in Fig.12 are the curves that offer the best compromise for each grouping studied for the second stage. Fi.13 does not include cases where the nodes are less than 100 since it offers BER values considerably higher than the other cases analyzed. Based on what we found, we can say that the 300 and 400 nodes on the BER curves for the second stage give the best results compared to the SNR. Because 400 nodes in the second stage indicate that only a small number of nodes make up the central node, the second stage of our approach will include testing with groups of 300 and 400 nodes. In light of this, the parameters of e have been set to 7, 8, 9, 10, and 11 for this method's 100, 200, 300, and 400 HADs groups. Table 12 shows the *DD*s that correlate to these curves. The values are quite higher than they were in other situations examined.

When analyzing the curves obtained in Fig. 12, it is seen that the slope of the BER-SNR curve in the Waterfall region increases when a greater number of nodes per group is used. This is because by increasing the number of nodes involved in the encoding, the generator matrix code becomes more dispersed, which causes the LDPC codes to have better properties. In the same way, lower BER values are also obtained for groups with a greater number of HAD nodes.

The response corresponding to each packet is elaborated by randomly choosing three correctly received packets. By analyzing the curve in Fig.12, it is clear that the slope of the curve in the BER-SNR in the waterfall region increases when more HDA nodes are used for the group. The LDPC code is a little dispersed and offers poor performance.

Similarly, we obtained some values of less BER in the case of HAD with the highest number of nodes. This supposition is because when increasing the number of nodes that intervene in the coding, the generator matrix of the code becomes more dispersed, which leads to LPDC codes having better properties. When BER-SNR curves from distributed LDPC coding (second stage level algorithm shown) are compared, the second stage algorithm is a better compromise.

Given the results, it can be concluded that the best BER versus SNR curves for the second stage correspond to groups of 300 HDAs and 400 HDAs. As 400 HDAs in the second stage imply that the number of central nodes is very low, we will try groups of 300 HDAs and 400 HDAs for the third stage of the proposed PHA.

In the third stage of the algorithm, each central node sends all the packets received in its group. The third stage will be carried out assuming that the total nodes of the network are 1200 HDAs. Therefore, by dividing it into four groups of 300 HDAs, there is a total of 4 central nodes, and if it is divided into 12 groups of 100 HDAs, there is a total of 12 CNs.

C. THIRD STAGE: IDEAL CASE

We analyze the ideal case of this third stage for 1200 HDAs in total. The basic purpose of this section is to determine

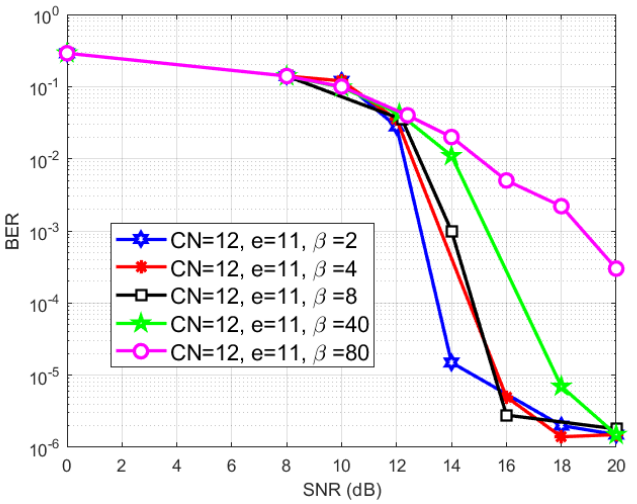

FIGURE 14. BER-SNR curve obtained for a distributed LDPC coding (third stage of the presented algorithm) in a smart lab network of 1200 HDAs, with 12 CNs and parameter value $e = 12$.The maximum number of iterations of the decoding algorithm is 10, and the value of β is 2, 4, 8, 40, and 80 packets per burst.

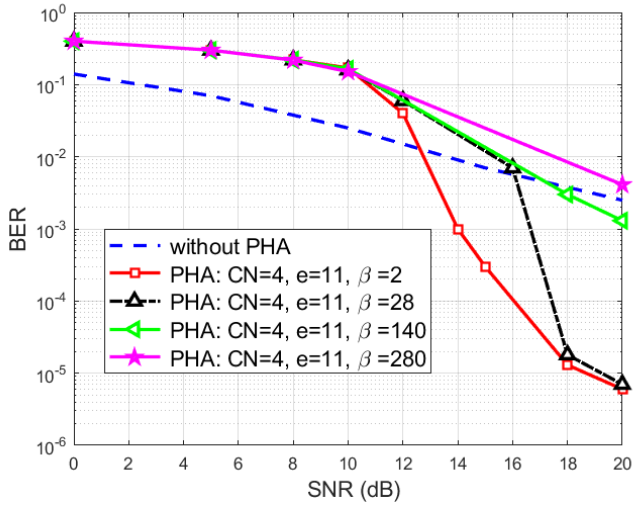

FIGURE 15. BER-SNR curve, the value of is 2, 28, 140, and 280 packets per burst with four CNs (400 nodes per subnet).

the appropriate values for the parameter e to improve the algorithm's performance in the third stage (as seen in Figs 13,14 and 15).

In Fig.15, we present the curve obtained under ideal conditions, considering the assumptions described for this scenario. The simulation includes a total of 1200 nodes transmitting a single packet. We have equated the burst size to a symbol of time. The decoding algorithm's maximum number of iterations has been set at ten, consistent with the third stage. The values of parameter e have varied between 10 and 13; for $e = 12$ and $e = 13$, the curves offered a better compromise. For the third stage scenarios, an analysis will be carried out for different gust sizes with $e = 12$ and $e = 13$.

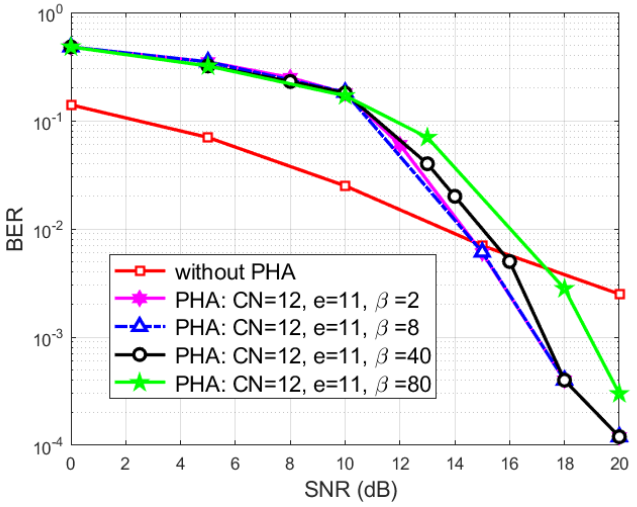

FIGURE 16. BER-SNR curve the value of $e = 11$ and $\beta = 2, 8, 40,$ *and* 80 packets per burst with 12 CNs (100 HAD nodes per group).

This case is equivalent to studying a second stage in which the size of all subnets is 1200 nodes. From this case, it is possible to extract the good values of the parameter e and use them in the encoding in this third stage. For the third stage, the coherence time of the channels should have a very small value.

D. RESULTS ANALYSIS OF THE COMPLETE SYSTEM

In this subsection, we will analyze the results of the complete system from the data obtained for the algorithm's first, second, and third stages. The objective is to see the final behavior of the BER versus SNR curves after both hops and compare it with the case of not using PHA. The results obtained after both phases in the third stage are compared in Fig.16 for the scenario of separating the HDA nodes into 12 CNs 100 HDA nodes each with $e = 11$ and burst sizes of β=2,8,40, and 80 packets per burst, as well as the situations of not utilizing PHA. The maximum number of iterations of the algorithm decoding is 10, Fig.16 shows the BER-SNR curve obtained for distributed LDPC coding schemes through the proposed algorithm's first, second, and third stages.

Fig. 16 shows how an improvement is obtained when using the proposed algorithm at high SNR values (close to 15 dB) for all burst sizes, compared to the case of not using encoding, with an improvement point close to 15 dB. Except in the case where $\beta = 80$, the results for these values are worse than those for the 4 CNs of 300 *HDA*s. It is necessary to go to SNR values greater than 16 dB to obtain an improvement using the proposed algorithm concerning multihop LDPC, obtained for an SNR of 16 dB and using burst sizes equivalent to $\beta = 2$. Coding gains of close to 7 dB compared to the case without encryption. If this coding gain is calculated to be 20 dB, the gains for bursts of size $\beta = 2$ are 17 dB compared to the case where there is no coding and 13 dB compared to the case where there is multihop LDPC coding. Furthermore, for an

TABLE 12. A summary of the improvement Point in dB of the results obtained from the entire system ($e = 11$ HDA=300 and CN=4):.

Burst Size (β)	Improvement Points in dB
$\beta = 2$	17
$\beta = 8$	13
$\beta = 40$	11
$\beta = 80$	10

SNR of 20 dB, the coding gain obtained in the case where the burst is of size $\beta = 80$ is 10 dB compared to the case without coding and 7 dB compared to the multihop LDPC coding, indicating that with these SNR values, our algorithm has a significant advantage in the two scenarios analyzed (300 and 100 HDAs per subnet).

Finally, the system's results were analyzed using data from the proposed algorithm's three stages. The objective was to observe the BER curves' behavior against SNR after both hops and compare it with the case of not using LDPC and NC, determining the improvement point in dB. Additionally, we compiled a comprehensive summary table highlighting our study's significant results and implications. This table will be a valuable resource for other experts in the field, facilitating their access to and application of our findings in their research and practice.

These results show the improvement in coding gain achieved by using the proposed algorithm compared to not using coding or using the multihop LDPC algorithm. The table presents the improvement in dB for different burst sizes (β). The proposed algorithm consistently outperforms the other schemes, especially at higher SNR values.

VIII. CONCLUSION

This research paper proposes a new PHA for real-time control of multiple virus vaccine types in a smart laboratory setting. The algorithm aims to improve the BER in dense wireless medical sensor networks and ensure the reliable relay of big data in healthcare. The PHA consists of three main creation stages: collecting big medical data, utilizing coding approaches based on NC and LDPC, and reducing BER in deep fading environment receivers. The proposed algorithm leverages the IoMT to track the evolution of virus vaccines and select the best one. The study highlights the importance of effective communication schemes, NC, and LDPC coding techniques in improving BER and minimizing communication delays in wireless IoT networks. The results show promising performance gains and coding advantages compared to non-coding scenarios. Using groups or subnets with many nodes is recommended for better system performance. This research advances healthcare communication systems and vaccine testing in smart laboratories.

REFERENCES

[1] A. Asadi, Q. Wang, and V. Mancuso, "A survey on device-to-device communication in cellular networks," *IEEE Commun. Surveys Tuts.*, vol. 16, no. 4, pp. 1801–1819, 4th Quart., 2014.

[2] I. W. G. D. Silva, J. D. V. Sanchez, E. E. B. Olivo, and D. P. M. Osorio, "Impact of self-energy recycling and cooperative jamming on SWIPT-based FD relay networks with secrecy constraints," *IEEE Access*, vol. 10, pp. 24132–24148, 2022, doi: 10.1109/ACCESS.2022.3155498.

[3] M. Abolhasan, J. Lipman, W. Ni, and B. Hagelstein, "Software-defined wireless networking: Centralized, distributed, or hybrid?" *IEEE Netw.*, vol. 29, no. 4, pp. 32–38, Jul. 2015.

[4] L. F. M. Vieira, M. Gerla, and A. Misra, "Fundamental limits on end-to-end throughput of network coding in multi-rate and multicast wireless networks," *Comput. Netw.*, vol. 57, no. 17, pp. 3267–3275, Dec. 2013.

[5] E. M. Ar-Reyouchi, Y. Chatei, K. Ghoumid, M. Hammouti, and B. Hajji, "Efficient coding techniques algorithm for cluster-heads communication in wireless sensor networks," *AEU-Int. J. Electron. Commun.*, vol. 82, pp. 294–304, Dec. 2017.

[6] E. M. Ar-Reyouchi, A. Lichioui, and S. Rattal, "A group cooperative coding model for dense wireless networks," *Int. J. Adv. Comput. Sci. Appl.*, vol. 10, no. 7, pp. 367–373, 2019, doi: 10.14569/IJACSA.2019.0100750.

[7] R. Prior, D. E. Lucani, Y. Phulpin, M. Nistor, and J. Barros, "Network coding protocols for smart grid communications," *IEEE Trans. Smart Grid*, vol. 5, no. 3, pp. 1523–1531, May 2014.

[8] N. D. S. R. Junior, M. A. Vieira, L. F. Vieira, and O. Gnawali, "CodeDrip: Data dissemination protocol with network coding for wireless sensor networks," in *Proc. Eur. Conf. Wireless Sensor Netw.*, Cham, Switzerland: Springer, 2014, pp. 34–49.

[9] Y. Lamrani, I. Benchaib, K. Ghoumid, and E. M. Ar-Reyouchi, "A new coded diversity combining scheme for high microwave throughput," in *Intelligent Data Communication Technologies and Internet of Things*, vol. 101. Coimbatore, India: Springer, 2022, doi: 10.1007/978-981-16-7610-9_50.

[10] R. Ahlswede, N. Cai, S.-Y. R. Li, and R. W. Yeung, "Network information flow," *IEEE Trans. Inf. Theory*, vol. 46, no. 4, pp. 1204–1216, Jul. 2000.

[11] S. Jaggi, P. Sanders, P. A. Chou, M. Effros, S. Egner, K. Jain, and L. M. G. M. Tolhuizen, "Polynomial time algorithms for multicast network code construction," *IEEE Trans. Inf. Theory*, vol. 51, no. 6, pp. 1973–1982, Jun. 2005.

[12] E. M. Ar Reyouchi, K. Ameziane, O. El Mrabet, and K. Ghoumid, "The potentials of network coding for improvement of round trip time in wireless narrowband RF communications," in *Proc. Int. Conf. Multimedia Comput. Syst. (ICMCS)*, Apr. 2014, pp. 765–770.

[13] Z. Guo, B. Wang, P. Xie, W. Zeng, and J. H. Cui, "Efficient error recovery with network coding in underwater sensor networks," *Ad Hoc Netw.*, vol. 7, no. 4, pp. 791–802, Jun. 2009, doi: 10.1016/j.adhoc.2008.07.011.

[14] X. Bao and J. Li, "Matching code-on-graph with network-on-graph: Adaptive network coding for wireless relay networks," in *Proc. Allerton Conf. Commun. Control Comput.*, 2005.

[15] X. Bao and J. Li, "Adaptive network coded cooperation (ANCC) for wireless relay networks: Matching code-on-graph with network-on-graph," *IEEE Trans. Wireless Commun.*, vol. 7, no. 2, pp. 574–583, Feb. 2008, doi: 10.1109/TWC.2008.060439.

[16] R. Gallager, "Low-density parity-check codes," *IRE Trans. Inf. Theory*, vol. 8, no. 1, pp. 21–28, Jan. 1962, doi: 10.1109/TIT.1962.1057683.

[17] T. Patra and S. Sil, "Bit error rate performance evaluation of different digital modulation and coding techniques with varying channels," in *Proc. 8th Annu. Ind. Autom. Electromechanical Eng. Conf. (IEMECON)*, Aug. 2017, pp. 4–10, doi: 10.1109/IEMECON.2017.8079551.

[18] M. Hammouti, E. M. Ar-Reyouchi, K. Ghoumid, and A. Lichioui, "Clustering analysis of wireless sensor network based on network coding with low-density parity check," *Int. J. Adv. Comput. Sci. Appl.*, vol. 7, no. 3, pp. 137–143, Mar. 2016.

[19] S. Abdul-Nabi, A. Khalil, P. Mary, and J.-F. Hélard, "Efficient network coding solutions for limiting the effect of packet loss," *EURASIP J. Wireless Commun. Netw.*, vol. 2017, no. 1, p. 35, Dec. 2017, doi: 10.1186/s13638-017-0817-3.

[20] S. Lin and D. J. Costello, *Error Control Coding: Fundamentals and Applications*. Upper Saddle River, NJ, USA: Prentice-Hall, 1983, ch. 15.

[21] K. Kotuliaková, D. Simlastíková, and J. Polec, "Analysis of ARQ schemes," *Telecommun. Syst.*, vol. 52, no. 3, pp. 1677–1682, Mar. 2013.

[22] E. M. A. Reyouchi, Y. Chatei, K. Ghoumid, and A. Lichioui, "The powerful combined effect of forward error correction and automatic repeat request to improve the reliability in the wireless communications," in *Proc. Int. Conf. Comput. Sci. Comput. Intell. (CSCI)*, Dec. 2015, pp. 691–696.

[23] H. Zhu, M. Li, I. Chlamtac, and B. Prabhakaran, "A survey of quality of service in IEEE 802.11 networks," *IEEE Wireless Commun.*, vol. 11, no. 4, pp. 6–14, Aug. 2004.

[24] L. Hanzo and R. Tafazolli, "A survey of QoS routing solutions for mobile ad hoc networks," *IEEE Commun. Surveys Tuts.*, vol. 9, no. 2, pp. 50–70, 2nd Quart., 2007.

[25] P. Chen, L. Shi, S. C. Liew, Y. Fang, and K. Cai, "Channel decoding for nonbinary physical-layer network coding in two-way relay systems," *IEEE Trans. Veh. Technol.*, vol. 68, no. 1, pp. 628–640, Jan. 2019.

[26] S. Katti, H. Rahul, W. Hu, D. Katabi, M. Medard, and J. Crowcroft, "XORs in the air: Practical wireless network coding," in *Proc. Conf. Appl., Technol., Architectures, Protocols Comput. Commun.*, New York, NY, USA, 2006, pp. 243–254.

[27] J. Zhang, Y. P. Chen, and I. Marsic, "MAC-layer proactive mixing for network coding in multi-hop wireless networks," *Comput. Netw.*, vol. 54, no. 2, pp. 196–207, Feb. 2010.

[28] J. Le, J. C. S. Lui, and D. M. Chiu, "DCAR: Distributed coding-aware routing in wireless networks," in *Proc. 28th Int. Conf. Distrib. Comput. Syst.*, Washington, DC, USA, Jun. 2008, pp. 462–469.

[29] E. M. Ar-Reyouchi, M. Hammouti, I. Maslouhi, and K. Ghoumid, "The Internet of Things: Network delay improvement using network coding," in *Proc. 2nd Int. Conf. Internet Things, Data Cloud Comput.*, Cambridge, U.K., Mar. 2017, pp. 1–7, doi: 10.1145/3018896.3018902.

[30] T. Ho, R. Koetter, M. Medard, D. R. Karger, and M. Effros, "The benefits of coding over routing in a randomized setting," in *Proc. IEEE Int. Symp. Inf. Theory*, Yokohama, Japan, 2003, p. 442, doi: 10.1109/ISIT.2003.1228459.

[31] S.-Y. R. Li, R. W. Yeung, and N. Cai, "Linear network coding," *IEEE Trans. Inf. Theory*, vol. 49, no. 2, pp. 371–381, Feb. 2003.

[32] D. Chen, B. Rong, N. Shayan, M. Bennani, J. Cabral, M. Kadoch, and A. K. Elhakeem, "Interleaved FEC/ARQ coding for QoS multicast over the internet," *Can. J. Electr. Comput. Eng.*, vol. 29, no. 3, pp. 159–166, Jul. 2004, doi: 10.1109/CJECE.2004.1532519.

[33] A. Al-Fuqaha, M. Guizani, M. Mohammadi, M. Aledhari, and M. Ayyash, "Internet of Things: A survey on enabling technologies, protocols, and applications," *IEEE Commun. Surveys Tuts.*, vol. 17, no. 4, pp. 2347–2376, 4th Quart., 2015, doi: 10.1109/COMST.2015.2444095.

[34] C. E. Shannon, "A mathematical theory of communication," *Bell Syst. Tech. J.*, vol. 27, pp. 379–423, Jul. 1948. [Online]. Available: http://cm.bell-labs.com/ cm/ms/what/shannonday/shannon1948.pdf

[35] P. A. Chou, Y. Wu, and K. Jain, "Practical network coding," in *Proc. 41st Annu. Allerton Conf. Commun., Controls, Computations*, Monticello, IL, USA, Oct. 2003, pp. 1–10.

[36] V. A. Vasudevan, T. Akhtar, C. Tselios, I. Politis, and S. Kotsopoulos, "Study of secure network coding enabled mobile small cells," in *Proc. IEEE Int. Conf. Commun.*, Jun. 2021, pp. 1–5, doi: 10.1109/ICC42927.2021.9500614.

[37] T. Ho, R. Koetter, M. Medard, D. R. Karger, and M. Effros, "The benefits of coding over routing in a randomized setting," in *Proc. IEEE Int. Symp. Inf. Theory*, Yokohama, Japan, 2003, p. 442, doi: 10.1109/ISIT.2003.1228459.

[38] T. Ho, M. Médard, J. Shi, M. Effros, and D. R. Karger, "On randomized network coding," in *Proc. Annu. Allerton Conf. Commun. Control Comput.*, 2003, vol. 41, no. 1, pp. 11–20.

[39] J.-S. Park, M. Gerla, D. Lun, Y. Yi, and M. Medard, "Codecast: A network-coding-based ad hoc multicast protocol," *IEEE Wireless Commun.*, vol. 13, no. 5, pp. 76–81, Oct. 2006.

[40] C. C. Chen, S. Y. Oh, P. Tao, M. Gerla, and M. Y. Sanadidi, "Pipeline network coding for multicast streams," in *Proc. Int. Conf. Mobile Comput. Ubiquitous Netw.*, 2010, pp. 1–7.

[41] C.-C. Chen, C. Chen, S. Y. Oh, J.-S. Park, M. Gerla, and M. Y. Sanadidi, "ComboCoding: Combined intra-/inter-flow network coding for TCP over disruptive MANETs," *J. Adv. Res.*, vol. 2, no. 3, pp. 241–252, Jul. 2011.

[42] D. Nguyen, T. Tran, T. Nguyen, and B. Bose, "Wireless broadcast using network coding," *IEEE Trans. Vehicular Technol.*, vol. 58, no. 2, pp. 914–925, Feb. 2009, doi: 10.1109/TVT.2008.927729.

[43] D. Nguyen, T. Tran, T. Nguyen, and B. Bose, "Wireless broadcast using network coding," *IEEE Trans. Veh. Technol.*, vol. 58, no. 2, pp. 914–925, Feb. 2009.

[44] G. Sarkis, J. B. Soriaga, and T. Richardson, "Self-decodability of HARQ retransmissions for 5G NR LDPC codes," in *Proc. 11th Int. Symp. Topics Coding (ISTC)*, Aug. 2021, pp. 1–5, doi: 10.1109/ISTC49272.2021.9594241.

[45] M. Ghaderi, D. Towsley, and J. Kurose, "Reliability gain of network coding in lossy wireless networks," in *Proc. IEEE INFOCOM 27th Conf. Comput. Commun.*, Apr. 2008, pp. 196–200.

[46] Y. Kondo, H. Yomo, S. Yamaguchi, P. Davis, R. Miura, and S. Obana, "Reliable wireless broadcast with random network coding for real-time applications," in *Proc. IEEE Wireless Commun. Netw. Conf.*, Budapest, Hungary, Apr. 2009, pp. 1–6.

[47] E. Rozner, A. P. Iyer, Y. Mehta, L. Qiu, and M. Jafry, "ER: Efficient retransmission scheme for wireless LANs," in *Proc. ACM CoNEXT Conf.*, 2007, pp. 1–12.

[48] E. M. Ar-Reyouchi, K. Ghoumid, D. Ar-Reyouchi, S. Rattal, R. Yahiaoui, and O. Elmazria, "Protocol wireless medical sensor networks in IoT for the efficiency of healthcare," *IEEE Internet Things J.*, vol. 9, no. 13, pp. 10693–10704, Jul. 2022, doi: 10.1109/JIOT.2021.3125886.

[49] T. Q. S. Quek, D. Dardari, and M. Z. Win, "Energy efficiency of dense wireless sensor networks: To cooperate or not to cooperate," *IEEE J. Sel. Areas Commun.*, vol. 25, no. 2, pp. 459–470, Feb. 2007.

[50] Z. Ren, Y.-D. Wen, and Y.-K. Yao, "An improved wireless broadcasting retransmission approach based on network coding," in *Proc. 8th Int. Conf. Wireless Commun., Netw. Mobile Comput.*, Sep. 2012, pp. 1–4.

[51] S. Katti, H. Rahul, W. Hu, D. Katabi, M. Medard, and J. Crowcroft, "XORs in the air: Practical wireless network coding," *IEEE/ACM Trans. Netw.*, vol. 16, no. 3, pp. 497–510, Jun. 2008.

[52] S. Sengupta, S. Rayanchu, and S. Banerjee, "An analysis of wireless network coding for unicast sessions: The case for coding-aware routing," in *Proc. IEEE INFOCOM 26th IEEE Int. Conf. Comput. Commun.*, May 2007, pp. 1028–1036.

[53] J. Garcia-Frias and W. Zhong, "Approaching Shannon performance by iterative decoding of linear codes with low-density generator matrix," *IEEE Commun. Lett.*, vol. 7, no. 6, pp. 266–268, Jun. 2003, doi: 10.1109/LCOMM.2003.813816.

[54] T. J. Richardson and R. L. Urbanke, "Efficient encoding of low-density parity-check codes," *IEEE Trans. Inf. Theory*, vol. 47, no. 2, pp. 638–656, Feb. 2001, doi: 10.1109/18.910579.

[55] D. J. C. MacKay, "Good error-correcting codes based on very sparse matrices," *IEEE Trans. Inf. Theory*, vol. 45, no. 2, pp. 399–431, Mar. 1999, doi: 10.1109/18.748992.

[56] J. Proakis, *Digital Communications*, 4th ed. New York, NY, USA: McGraw-Hill, Aug. 2000.

[57] T. Tian, C. Jones, J. D. Villasenor, and R. D. Wesel, "Construction of irregular LDPC codes with low error floors," in *Proc. IEEE Int. Conf. Commun.*, May 2003, pp. 3125–3129.

EL MILOUD AR-REYOUCHI (Senior Member, IEEE) received the engineering degree from the Institute National of Post and Telecommunication (INPT), Rabat, Morocco, the M.S. degree in industrial computer, the C.P.D. degree in automatic and industrial computer and the D.E.A. degree in computer engineering from the Department of Computer Science and Control, as well as the D.E.A. degree from the Department of Telecommunication and Computer Science, Madrid, Spain. Additionally, he obtained a Ph.D. degree in Telecommunication and Computer Science from Abdelmalek Essaadi University, Tétouan, Morocco. He is currently with the Department of Telecommunication and Computer Science, and the Service Regional Head of the Radio and Television Broadcast Station at Société Nationale de Radiodiffusion et de Télévision (SNRT), Morocco. His research interests include telecommunication, broadcasting TV/FM, engineering automatic systems, mobile wireless networks, the Internet of Things, wireless communications, broadcasting TV/radio FM, antennas, propagation, and wireless devices for medical communication systems and sensing applications.

GUNJAN VARSHNEY (Senior Member, IEEE) received the M.Tech. degree (Hons.) in electrical power and energy systems from UPTU Lucknow, India, and the Ph.D. degree from Uttarakhand Technical University, Dehradun. She is currently pursuing the engineering degree (Hons.) in electrical engineering from the Government Engineering College, Kota, India. She is also a Branch Counselor with the IEEE JSS Academy of Technical Education (JSSATEN) Student Branch, Noida. She is also the WIE IEEE JSSATEN Student Branch's Faculty Advisor. She won the university gold medal in master's degree. She has 18 years of experience in total. She spent over 15 years working for JSSATEN. She has more than 30 of her research papers have been published in journals and conferences at both the national and international levels. She plans conferences, seminars, training and internship programs, SDPs, and FDPs. Her research interests include DC distribution systems and microgrids, renewable energy sources, and power quality problems and solutions. She contributes to the MDSM Committee of the IEEE UP Section.

KAMAL GHOUMID (Member, IEEE) received the engineering degree in electronics and telecommunications from CNAM, Paris, France, the joint master's degree in technics of radiocommunications and in research master communication systems from Gustave Eiffel University and Paris-Est University, France, the joint Ph.D. degree from Institut FEMTO-ST, Bourgogne Franche-Comté University, Besançon, France, and Télécom SudParis de l'Institut Polytechnique de Paris, Evry, France, in 2008, and the joint Diploma (Habilitation à Diriger des Recherches) (H.D.R.) degree from Sorbonne University and Pierre-et-Marie-Curie University, France, in 2020. He was a Postdoctoral Researcher with the Jean Lamour Institute of Lorraine University, Nancy, France, from 2008 to 2009, and the FEMTO-ST Institute, Bourgogne Franche-Comté University. Currently, he is a Professor with the National School of Applied Sciences (ENSAO), Mohammed Premier University, Oujda, Morocco. At the start of these research activities, he worked on integrated components dedicated to optical telecommunications systems (optical filtering and modulations) and radio-over-fiber applications. His current research interests include digital communications, the Internet of Things, and wireless and optical communications. He also has good experience in antennas and propagation research areas.

FABIEN PICAUD received the Ph.D. degree from the University of Franche Comte, in 2001. He has been a lecturer, since 2004, after one postdoctoral position at the international superior school of advanced studies—SISSA, Trieste, Italy. He is currently the Co-Director of Laboratoire de Nanomédecine, Imagerie et Thérapeutiques, and the Director of the Mesocentre of Calculations of Franche Comté. His research interests include computing in natural science, engineering and medicine, distributed computing, and molecular physics. His main topic concerns algorithm development in several domains dedicated to medical science. More particularly, he is in the role of confinement on the stability of different molecular species inside nanostructures to develop the medicine of tomorrow at the nanoscale.

GUILLAUME HERLEM received the Graduate degree from the University of Pierre and Marie Curie, Paris 6, France, in 1994, and the Ph.D. degree in physical chemistry from the University of Franche-Comte, in 1997. He has been an Assistant Professor (authorized to direct research) in physical chemistry with the University of Franche-Comte, France, since 1998. Up to now, he has supervised 16 Ph.D. students in physical chemistry but with a multidisciplinary orientation, such as energy storage (secondary batteries and supercapacitors) and biosensors embedded in MEMs. In 2012, he actively created a new multidisciplinary laboratory in nanomedicine, gathering physicists, chemists, physicians, and pharmacists. Since this date, he has been developing innovative therapies in medicine, such as nanovectors embedding TRAIL cytokine against cancer cells for drug delivery, biomonitoring nosocomial diseases, fall tracking and health monitoring in the elderly, and modelizations. He is also involved with applied research, participated in several industrial projects, and authored ten patents.

AHMED MOSTEFAOUI received the M.S. and Ph.D. degrees in computer science from Ecole Normale Superieure de Lyon, France, in 1996 and 2000, respectively. He has been an Associate Professor with the University of Franche Comte, France, since 2000. His research interests include distributed algorithms in wireless ad-hoc and sensor networks, emphasizing practical and theoretical issues, multimedia systems, and networking, particularly distributed architectures.

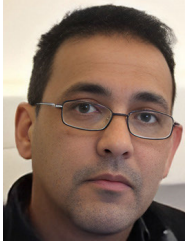

RÉDA YAHIAOUI received the engineering degree in electronics from USTHB-Algeria, in 1993, the Diploma of Advanced Studies (D.E.A.) degree in electronics, sensors and integrated circuits—microwave and fast electronics option, in 1998, and the Ph.D. degree in engineering science from the University of Paris-XI, Orsay, in 2002. Since September 2005, he has been a Lecturer with the Electronics Department, University of Franche Comté, and UFR-ST, Besançon, for the teaching mission; he was attached for the research mission to the MN2S Department, FEMTO-ST Institute, until April 2019, where he joined the LNIT Laboratory. His research interests include developing BioMEMS devices for biomedical applications, particularly vibrating MEMS for detecting bacteria in healthcare establishments and intelligent monitoring systems connected remotely, capable of monitoring health and preventing illnesses. He falls at home or in institutions for the elderly.